

# Where the linearized Poisson-Boltzmann cell model fails: (II) the planar case as a prototype study

M. N. Tamashiro and H. Schiessel  
*Max-Planck-Institut für Polymerforschung,  
 Ackermannweg 10, 55128 Mainz, Germany*

## Abstract

The classical problem of two uniformly charged infinite planes in electrochemical equilibrium with an infinite monovalent salt reservoir is solved exactly at the mean-field nonlinear Poisson-Boltzmann (PB) level, including an explicit expression of the associated nonlinear electrostatic contribution to the semi-grand-canonical potential. A linearization of the nonlinear functional is presented that leads to Debye-Hückel-like equations agreeing asymptotically with the nonlinear PB results in the weak-coupling (high-temperature) and counterionic ideal-gas limits. This linearization scheme yields artifacts in the low-temperature, large-separation or high-surface charge limits. In particular, the osmotic-pressure difference between the interplane region and the salt reservoir becomes negative in the above limits, in disagreement with the exact (at mean-field level) nonlinear PB solution. By using explicitly gauge-invariant forms of the electrostatic potential we show that these artifacts — although thermodynamically consistent with quadratic expansions of the nonlinear functional — can be traced back to the non-fulfillment of the underlying assumptions of the linearization. Explicit comparison between the analytical expressions of the exact nonlinear solution and the corresponding linearized equations allows us to show that the linearized results are asymptotically exact in the weak-coupling and counterionic ideal-gas limits, but always fail otherwise, predicting negative osmotic-pressure differences. By taking appropriate limits of the full nonlinear PB solution, we provide asymptotic expressions for the semi-grand-canonical potential and the osmotic-pressure difference that involve only elementary functions, which cover the complementary region where the linearized theory breaks down.

## 1 Introduction

In the preceding paper<sup>1</sup> we performed a linearization of the mean-field Poisson-Boltzmann (PB) density functional for spherical Wigner-Seitz cells that agrees asymptotically with the PB results in the weak-coupling (high-temperature) limit by adopting an explicitly gauge-invariant approach. However, as already pointed out previously in the literature,<sup>2,3</sup> the linearization scheme yields artifacts in the low-temperature, high-surface charge or infinite-dilution (of polyions) limits for the Donnan equilibrium problem<sup>4,5,6,7,8</sup> in spherical geometry, which describes a suspension of spherical charged polyions in electrochemical equilibrium with an infinite salt reservoir. In these limits the linearized osmotic-pressure difference between the colloidal suspension and the salt reservoir becomes negative, in disagreement with the full nonlinear PB result, that always displays positive osmotic-pressure differences. Because the nonlinear PB equation is not analytically solvable in spherical geometry — even in the simplest salt-free case, when only neutralizing counterions are present — one must rely on numerical calculations to establish comparisons between the nonlinear and the linearized equations. This motivated us to consider the prototype case represented by the classical problem of two uniformly charged infinite planes in electrochemical equilibrium with an infinite salt reservoir, when the exact analytical solution of the nonlinear problem is possible. The explicit analytical comparison between the exact (at the mean-field level) full nonlinear and the approximated linearized equations allows us to trace back the underlying reasons of the breakdown of the linearization scheme that is intrinsically associated with its range of validity. Additionally, the study of this exactly-solvable case sheds some light on the question of the proper definition of the linearized osmotic pressure that was previously considered in Ref. [3].

Moreover, to our knowledge, the explicit calculation of the semi-grand-canonical potential for two uniformly charged infinite planes at the nonlinear mean-field PB level has only been reported in connection

to the polyelectrolyte-brush problem.<sup>9</sup> In that work, however, the thermodynamical potential also included electrostatic and elastic contributions arising from the polyelectrolyte brushes, and therefore, these need to be subtracted out. The knowledge of the thermodynamic potential allows us to derive all thermodynamic properties of the two charged infinite planes problem. We note that it can be also extended to curved surfaces by using the Derjaguin approximation.<sup>10, 11, 12</sup> It is then possible to determine the normal forces (per unit area) between these surfaces when their separation distance is much smaller than their curvature radius. We will present the exact nonlinear semi-grand-canonical functional from which we derive approximate expressions. These involve only elementary functions and provide excellent approximations to the full nonlinear PB results within the whole range of parameters.

The remainder of the paper is organized as follows. In Section 2 the model is introduced and the exact nonlinear solution is obtained. In Section 3 the linearization of the appropriate semi-grand-canonical functional is performed. In Section 4 we present explicit analytic comparisons between the exact nonlinear and the linearized equations of state. In Section 5 we give some concluding remarks. In Appendix A we compare the exact nonlinear and the self-consistent linearized averaged densities used to perform the quadratic expansion of the nonlinear functional. In Appendix B we derive the asymptotic expansions of the exact nonlinear solution. In Appendix C we obtain extended expansions of the exact nonlinear solution that are valid in the Gouy-Chapman (high-surface charge) and the large-separation limits, regions where the linearization scheme breaks down. In Appendix D we present linearized equations that preserve the exactness of the Legendre transformation between the semi-grand-canonical and canonical-ensemble formulations of the problem.

## 2 Exact nonlinear Poisson-Boltzmann solution

The system to be considered is comprised of two infinite planar surfaces a distance  $2L$  apart, each with surface charge  $-\sigma q$ , where  $q > 0$  is the elementary charge, in electrochemical equilibrium with an infinite monovalent salt reservoir of bulk salt density  $n_b$ . The microions (positive counterions and salt ions) are free to move in the region  $-L < x < L$  between the two charged surfaces, where we introduced a Cartesian axis perpendicular to the planes in which the midplane is located at  $x = 0$  and the two charged planes at  $x = \pm L$ . At the mean-field level of approximation the ions are treated as inhomogeneous ideal gases described by their average local number densities  $n_{\pm}(x)$ . We do not distinguish between (positive) counterions and positive ions derived from the salt dissociation. The total charge number density (counterions, salt ions and the negative surface charge on the planes) of the system,

$$\rho(x) = n_+(x) - n_-(x) - \sigma\delta(x+L) - \sigma\delta(x-L), \quad (1)$$

where  $\delta$  is the one-dimensional Dirac delta-function, is related to the reduced electrostatic potential  $\psi(x) \equiv \beta q \Psi(x)$ , which satisfies the (exact) Poisson equation,

$$\frac{d^2\psi(x)}{dx^2} = -4\pi\ell_B\rho(x), \quad (2)$$

where  $\ell_B \equiv \beta q^2/\epsilon$  is the Bjerrum length and  $\beta^{-1} = k_B T$  is the thermal energy. It is implicitly assumed that the solvent dielectric constant  $\epsilon$  remains the same outside the region containing the salt solution ( $|x| > L$ ), so image-charge effects due to dielectric contrast are absent. The formal solution of the Poisson equation (2) may be written in terms of the one-dimensional Green function  $G_1(x, x_0)$ ,

$$\psi(x) = \lim_{\delta L \rightarrow 0^+} \ell_B \int_{L-\delta L}^{L+\delta L} dx_0 G_1(x, x_0) \rho(x_0), \quad \frac{d^2 G_1(x, x_0)}{dx^2} = -4\pi\delta(x - x_0), \quad (3)$$

which in turn allows us to express the mean-field semi-grand-canonical functional (for one charged plane) per unit area as

$$\frac{\beta\Omega}{A} = \lim_{\delta L \rightarrow 0^+} \frac{\ell_B}{2} \int_0^{L+\delta L} dx \int_0^{L+\delta L} dx_0 \rho(x) G_1(x, x_0) \rho(x_0) + \sum_{i=\pm} \int_0^L dx n_i(x) \{ \ln [n_i(x)\zeta_i^3] - 1 - \beta\mu_i \}$$

$$= \frac{1}{8\pi\ell_B} \int_0^L dx \left[ \frac{d\psi(x)}{dx} \right]^2 + \sum_{i=\pm} \int_0^L dx n_i(x) \left\{ \ln \left[ \frac{n_i(x)}{n_b} \right] - 1 \right\}, \quad (4)$$

where  $\zeta_{\pm}$  are the thermal de Broglie wavelengths of cations (including the positive counterions) and anions, respectively, and the (mean-field) microion chemical potentials  $\beta\mu_{\pm} = \ln(n_b\zeta_{\pm}^3)$  assume ideal gases of uniform density  $n_b$  for both types of ions in the infinite salt reservoir. The last equality results from integrating the electrostatic energy (per unit area) — the first term of Eq. (4) — by parts and using the fact that surface contributions vanish due to Gauss' law and the overall electroneutrality of the system,

$$\lim_{\delta L \rightarrow 0^+} \int_0^{L+\delta L} dx \rho(x) = 0, \quad \text{or} \quad \int_0^L dx [n_+(x) - n_-(x)] = \sigma. \quad (5)$$

The equilibrium density profiles are obtained by minimizing the PB semi-grand-canonical functional (4) under the charge-neutrality constraint (5),

$$\frac{\delta}{\delta n_{\pm}(x)} \left[ \frac{\Omega}{A} - \mu_{\text{el}} \lim_{\delta L \rightarrow 0^+} \int_0^{L+\delta L} dx \rho(x) \right] = 0, \quad (6)$$

where we introduced the Lagrange multiplier  $\mu_{\text{el}}$  to ensure the neutrality condition (5). This yields the Boltzmann-weighted ionic profiles,

$$n_{\pm}(x) = n_b \exp[\pm\beta\mu_{\text{el}} \mp \psi(x)], \quad (7)$$

and the Lagrange multiplier  $\mu_{\text{el}}$  is found by imposing the charge-neutrality condition (5),

$$e^{\pm\beta\mu_{\text{el}}} = \frac{\sqrt{n_c^2 + (2n_b)^2\alpha_+\alpha_-} \pm n_c}{2n_b\alpha_{\pm}} e^{\pm\langle\psi\rangle}, \quad (8)$$

$$\alpha_{\pm} = \left\langle e^{\pm\langle\psi\rangle \mp \psi(x)} \right\rangle, \quad (9)$$

where  $n_c = \sigma/L$  is the average density of counterions in the interplane region  $|x| < L$  and the brackets denote unweighted spatial averages over the volume available to the microions,

$$\langle \mathcal{X}(x) \rangle \equiv \frac{1}{L} \int_0^L dx \mathcal{X}(x). \quad (10)$$

In close analogy to the spherical case — cf. Appendix E of Ref. [1] — it is possible to write the nonlinear equilibrium density profiles in an explicitly gauge-invariant form by inserting the Lagrange multiplier (8) into the Boltzmann-weighted ionic profiles, Eqs. (7),

$$n_{\pm}(x) = \frac{\sqrt{n_c^2 + (2n_b)^2\alpha_+\alpha_-} \pm n_c}{2\alpha_{\pm}} e^{\pm\langle\psi\rangle \mp \psi(x)}. \quad (11)$$

By explicitly gauge-invariant we mean that the equilibrium profiles do not depend *explicitly* on a particular choice of the zero of the potential, because they depend only on the difference  $\langle\psi\rangle - \psi(x)$ . Henceforth *gauge-invariant* will be a short writing to *explicitly gauge-invariant*. In particular, in the salt-free ( $n_b \rightarrow 0$ ) limit, these gauge-invariant forms lead — in a direct and transparent way — to the vanishing coion profile,  $n_-(x) \equiv 0$ , and to the salt-free equilibrium counterion profile,  $n_+(x) = n_c e^{\langle\psi\rangle - \psi(x)} / \alpha_+$ .

The most commonly used gauge<sup>12,13</sup> is the one in which the charge-neutrality Lagrange multiplier is zero,  $\mu_{\text{el}} \equiv 0$ , which *does not correspond* to the gauge in which the electrostatic potential *at the infinite salt reservoir* vanishes.<sup>14</sup> Henceforth, to simplify the notation and the calculations we will use the standard gauge  $\mu_{\text{el}} \equiv 0$  to treat the *nonlinear problem*. We should keep in mind, however, that the fixed-gauge electrostatic potential  $\varphi(x) \equiv \psi(x) - \beta\mu_{\text{el}}$  will no longer be gauge-invariant: its value at a particular point

— let us say, at the midplane,  $\varphi_0 \equiv \varphi(x = 0)$ , or at the charged surfaces,  $\varphi_L \equiv \varphi(x = L)$  — will be determined by imposing the overall charge neutrality (5) in the whole system. They can no longer be chosen arbitrarily, in contrast to their gauge-invariant counterparts,  $\psi_0 \equiv \psi(x = 0)$  or  $\psi_L \equiv \psi(x = L)$ . In the gauge-invariant formulation, either  $\psi_0$  or  $\psi_L$  may be chosen arbitrarily — but not both *simultaneously* — because the difference  $\psi_L - \psi_0 = \varphi_L - \varphi_0$  must eventually be preserved.

In the standard gauge the nonlinear problem reduces into solving the usual PB equation for two charged infinite planes,<sup>12, 13, 15</sup>

$$\frac{d^2\varphi(x)}{dx^2} = \kappa_b^2 \sinh \varphi(x) + \frac{2}{\Lambda} [\delta(x + L) + \delta(x - L)], \quad n_{\pm}(x) = n_b e^{\mp\varphi(x)}, \quad (12)$$

with the appropriate boundary conditions,

$$\psi'(x = 0) = \varphi'(x = 0) = 0, \quad \text{and} \quad \psi'(x = \mp L) = \varphi'(x = \mp L) = \pm \frac{2}{\Lambda}, \quad (13)$$

the prime (') denoting differentiation with respect to the argument. We have introduced two length scales: the Debye screening length associated with the bulk density  $n_b$  of the infinite salt reservoir,

$$\kappa_b^{-1} \equiv \frac{1}{\sqrt{8\pi\ell_B n_b}}, \quad (14)$$

and the Gouy-Chapman<sup>16, 17</sup> length,

$$\Lambda \equiv \frac{1}{2\pi\ell_B\sigma}, \quad (15)$$

which gives the characteristic (algebraic) decay length of the counterion distribution (for a salt-free system) around an infinite charged plane with bare surface charge  $\sigma$ .

Using the mathematical identity

$$\frac{d^2\varphi(x)}{dx^2} = \frac{1}{2} \frac{d(\varphi')^2}{d\varphi}, \quad (16)$$

it is possible to integrate the nonlinear PB Eq. (12) exactly,

$$[\varphi'(x)]^2 = \kappa_b^2 [2 \cosh \varphi(x) - 2 \cosh \varphi_0], \quad (17)$$

$$\kappa_b |x| = \int_{\varphi(x)}^{\varphi_0} \frac{d\varphi}{\sqrt{2 \cosh \varphi - 2 \cosh \varphi_0}} = \frac{F \left( \arccos \left[ \frac{\sinh \frac{\varphi_0}{2}}{\sinh \frac{\varphi(x)}{2}} \right] \middle| 1 / \cosh^2 \frac{\varphi_0}{2} \right)}{\cosh \frac{\varphi_0}{2}}, \quad (18)$$

whose solution is written in terms of the midplane electrostatic potential  $\varphi_0 < 0$  and  $F(\varphi|m) = \int_0^\varphi d\theta / \sqrt{1 - m \sin^2 \theta}$  is the incomplete elliptic integral of the first kind.<sup>18, 19, 20, 21</sup> Applying the boundary conditions (13) yields

$$\frac{2}{\lambda} = \sqrt{2 \cosh \varphi_L - 2 \cosh \varphi_0}, \quad (19)$$

$$l = \int_{\varphi_L}^{\varphi_0} \frac{d\varphi}{\sqrt{2 \cosh \varphi - 2 \cosh \varphi_0}} = \frac{F \left( \arccos \left[ \frac{\sinh \frac{\varphi_0}{2}}{\sinh \frac{\varphi_L}{2}} \right] \middle| 1 / \cosh^2 \frac{\varphi_0}{2} \right)}{\cosh \frac{\varphi_0}{2}}, \quad (20)$$

where we defined the two dimensionless distances  $\lambda \equiv \kappa_b \Lambda$  and  $l \equiv \kappa_b L$ , and  $\varphi_L < \varphi_0 < 0$  is the surface electrostatic potential at the charged planes. Introducing the variable

$$t \equiv \sinh^2 \frac{\varphi_0}{2}, \quad (21)$$

which *a posteriori* will be identified with half of the (dimensionless) osmotic-pressure difference between the interplane region and the salt reservoir — cf. Eq. (33) — the two boundary conditions can be combined into the eigenvalue equation,

$$l\sqrt{1+t} = F \left[ \arctan \left( \frac{1}{\lambda\sqrt{t}} \right) \middle| \frac{1}{1+t} \right], \quad \text{or} \quad \lambda\sqrt{t} = \text{cs} \left( l\sqrt{1+t} \middle| \frac{1}{1+t} \right), \quad (22)$$

where  $\text{cs}(u|m) = \text{cn}(u|m)/\text{sn}(u|m)$  is the ratio of the cosine-amplitude and sine-amplitude Jacobi elliptic functions.<sup>18, 19, 20, 21</sup> The explicit exact solution of the nonlinear PB problem can then be written as

$$\varphi(x) = -2 \operatorname{arcsinh} \left[ \sqrt{t} / \operatorname{cn} \left( \kappa_b |x| \sqrt{1+t} \left| \frac{1}{1+t} \right. \right) \right], \quad |x| \leq L. \quad (23)$$

It should be remarked that the exact solution to the nonlinear PB problem may be cast in several equivalent forms. Verwey and Overbeek,<sup>22</sup> quoted by Hunter,<sup>23</sup> gave an alternative form for the implicit solution (18),

$$\begin{aligned} \kappa_b |x| &= l + 2e^{-\varphi_0/2} \left[ F \left( \operatorname{arcsin} e^{-(\varphi_L - \varphi_0)/2} \mid e^{-2\varphi_0} \right) - F \left( \operatorname{arcsin} e^{-[\varphi(x) - \varphi_0]/2} \mid e^{-2\varphi_0} \right) \right] \\ &= 2e^{-\varphi_0/2} \left[ K \left( e^{-2\varphi_0} \right) - F \left( \operatorname{arcsin} e^{-[\varphi(x) - \varphi_0]/2} \mid e^{-2\varphi_0} \right) \right], \end{aligned} \quad (24)$$

where  $K(m) = F(\pi/2|m)$  is the complete elliptic integral of the first kind,<sup>18, 19, 20, 21</sup> while Behrens and Borkovec's version<sup>24</sup> to the explicit solution (23) reads

$$\varphi(x) = \varphi_0 + 2 \ln \operatorname{cd} \left( e^{-\varphi_0/2} \kappa_b |x|/2 \mid e^{2\varphi_0} \right), \quad (25)$$

where  $\operatorname{cd}(u|m)$  is the  $\operatorname{cd}$  Jacobi elliptic function.<sup>18, 19, 20, 21</sup> However, none of these previous works presented the explicit expression for the nonlinear PB semi-grand-canonical potential  $\Omega \equiv \Omega[n_{\pm}(x)]_{\text{equil}}$ , which can be extracted from Ref. [9] by neglecting the electrostatic and elastic contributions arising from the polyelectrolyte brushes.

The dimensionless *excess*<sup>25</sup> semi-grand-canonical potential per unit area,

$$\omega(\lambda, l) \equiv \frac{\kappa_b}{2n_b} \left[ \frac{\beta\Omega(\Lambda, L)}{A} + 2n_b L \right], \quad (26)$$

may be evaluated inserting the exact nonlinear solution (23) into the semi-grand-canonical functional (4) and performing the integrations. After some tedious algebra, we obtain

$$\begin{aligned} \omega(\lambda, l) &= \frac{2}{\lambda} \left( 2 \coth \frac{\varphi_L}{2} - \varphi_L \right) + 4E \left( \arccos \left[ \sinh \frac{\varphi_0}{2} / \sinh \frac{\varphi_L}{2} \right] \mid 1 / \cosh^2 \frac{\varphi_0}{2} \right) \cosh \frac{\varphi_0}{2} \\ &\quad - 2F \left( \arccos \left[ \sinh \frac{\varphi_0}{2} / \sinh \frac{\varphi_L}{2} \right] \mid 1 / \cosh^2 \frac{\varphi_0}{2} \right) \sinh \frac{\varphi_0}{2} \tanh \frac{\varphi_0}{2}, \end{aligned} \quad (27)$$

$$\omega(\lambda, \infty) = -\frac{2}{\lambda} \varphi_{\infty} - 8 \sinh^2 \frac{\varphi_{\infty}}{4}, \quad (28)$$

where  $E(\varphi|m) = \int_0^{\varphi} d\theta \sqrt{1 - m \sin^2 \theta}$  is the incomplete elliptic integral of the second kind,<sup>18, 19, 20, 21</sup>  $\varphi_{\infty} < 0$  is the reduced electrostatic surface potential at the charged plane at infinite separation and  $\omega(\lambda, \infty)$  represents the nonlinear excess self-energy of the system. Using the relations

$$\cosh \varphi_L = 1 + 2t + \frac{2}{\lambda^2}, \quad \cosh \varphi_{\infty} = 1 + \frac{2}{\lambda^2}, \quad (29)$$

and the fact that  $\varphi_L < 0$  and  $\varphi_{\infty} < 0$ , the excess semi-grand-canonical potential  $\omega$  may be cast in a simpler form,

$$\omega(\lambda, l) = \frac{2}{\lambda} \operatorname{arccosh} \left( 1 + 2t + \frac{2}{\lambda^2} \right) - \frac{4}{\lambda} \sqrt{\frac{1 + \lambda^2(1+t)}{1 + \lambda^2 t}} + 4\sqrt{1+t} E \left[ \arctan \left( \frac{1}{\lambda\sqrt{t}} \right) \mid \frac{1}{1+t} \right] - 2tl, \quad (30)$$

$$\omega(\lambda, \infty) = \frac{2}{\lambda} \operatorname{arccosh} \left( 1 + \frac{2}{\lambda^2} \right) + 4 \left( 1 - \frac{1}{\lambda} \sqrt{1 + \lambda^2} \right). \quad (31)$$

As already pointed out in the introduction, besides its intrinsic relevance, the semi-grand-canonical potential for the planar case has also an important application: by using the Derjaguin approximation,<sup>10, 11, 12</sup> valid when the range of interactions<sup>26</sup> (of order  $\kappa_b^{-1}$ ) and the separation distance  $2L$  between the two curved surfaces are much smaller than their curvature radius  $a$ , it is possible to determine their normal force (per unit area)  $\mathcal{F}$  at separation  $2L$  by

$$\frac{1}{\kappa_b a} \mathcal{F}(L) = \frac{k_B T}{\ell_B} [\omega(\lambda, l) - \omega(\lambda, \infty)]. \quad (32)$$

Returning to the planar case, the osmotic-pressure difference  $\Delta P$  between the interplane region and the infinite salt reservoir can be written in terms of the midplane reduced electrostatic potential  $\varphi_0$ ,

$$\begin{aligned}\Pi &\equiv \frac{\beta\Delta P}{2n_b} = -\frac{1}{2n_b} \frac{d}{dL} \left[ \frac{\beta\Omega(\Lambda, L)}{A} + 2n_b L \right]_{\sigma, \ell_B, \mu_{\pm}} = -\frac{d\omega(\lambda, l)}{dl} = \frac{n_+(0) + n_-(0) - 2n_b}{2n_b} \\ &= 2 \sinh^2 \frac{\varphi_0}{2} = 2t,\end{aligned}\tag{33}$$

which may be obtained by taking the formal derivative of  $\omega$  with respect to  $l$ , similarly as performed in Appendix A of Ref. [1]. Eq. (33) is a mean-field version<sup>27</sup> of the boundary-density theorem, which states that the osmotic pressure is simply given by the sum of the microionic densities at the midplane (WS-cell boundary). This simple relation does not hold beyond the mean-field level because of finite ionic-size effects and the presence of microionic correlations between particles located in the different semi-spaces separated by the midplane — even though it still does for *one* charged plane with the electrolyte confined by a *neutral* midplane.<sup>28</sup> We restrict ourselves, however, to the nonlinear mean-field result (33), which clearly predicts that the osmotic-pressure difference  $\Pi$  *is always positive*.

We should remark that the nonlinear osmotic-pressure difference (33) may also be written in a gauge-invariant form using the gauge-invariant equilibrium density profiles (11),

$$\Pi = \left[ \sqrt{\left(\frac{2}{\lambda l}\right)^2 + \alpha_+ \alpha_-} + \frac{2}{\lambda l} \right] \frac{e^{\langle\psi\rangle - \psi_0}}{2\alpha_+} + \left[ \sqrt{\left(\frac{2}{\lambda l}\right)^2 + \alpha_+ \alpha_-} - \frac{2}{\lambda l} \right] \frac{e^{-\langle\psi\rangle + \psi_0}}{2\alpha_-} - 1,\tag{34}$$

where  $\psi_0$  is the *arbitrary* midplane electrostatic potential in the gauge-invariant formulation. It does not need necessarily to coincide with the midplane electrostatic potential  $\varphi_0 \equiv 2 \operatorname{arcsinh} \sqrt{\Pi/2}$  in the standard gauge  $\mu_{\text{el}} \equiv 0$ . The gauge-invariant form (34) of the nonlinear osmotic-pressure difference will be useful later, at the end of Section 3, when establishing a connection between its quadratic expansion about the average potential  $\langle\psi\rangle$  and its linearized counterpart (54).

### 3 Linearization scheme

To obtain the linearized semi-grand-canonical functional  $\Omega_{\text{DH}}[n_{\pm}(x)]$  we truncate the expansion of the PB nonlinear semi-grand-canonical functional  $\Omega[n_{\pm}(x)]$ , Eq. (4), up to second order in the differences  $n_{\pm}(x) - \langle n_{\pm}(x) \rangle$ , where  $\langle n_{\pm}(x) \rangle \equiv (1/L) \int_0^L dx n_{\pm}(x)$  are the (*a priori* unknown) average densities,

$$\begin{aligned}\frac{\beta\Omega_{\text{DH}}}{A} &= \frac{1}{8\pi\ell_B} \int_0^L dx \left[ \frac{d\psi(x)}{dx} \right]^2 + L \sum_{i=\pm} \langle n_i \rangle \left[ \ln \frac{\langle n_i \rangle}{n_b} - 1 \right] + \sum_{i=\pm} [\langle n_i \rangle \ln \langle n_i \rangle] \int_0^L dx \left[ \frac{n_i(x)}{\langle n_i \rangle} - 1 \right] \\ &\quad + \frac{1}{2} \sum_{i=\pm} \langle n_i \rangle \int_0^L dx \left[ \frac{n_i(x)}{\langle n_i \rangle} - 1 \right]^2.\end{aligned}\tag{35}$$

After minimization of the functional  $\Omega_{\text{DH}}[n_{\pm}(x)]$  with respect to the profiles  $n_{\pm}(x)$  under the overall electroneutrality constraint (5),  $[\delta/\delta n_{\pm}(x)] [\Omega_{\text{DH}}/A - \mu_{\text{el}} \int dx \rho(x)] = 0$  — analogously as performed for the spherical case in Appendix F of Ref. [1] — we obtain the self-consistent linearized averaged densities,

$$\bar{n}_{\pm} \equiv \langle n_{\pm}(x) \rangle_1 = \frac{\sqrt{n_c^2 + (2n_b)^2} \pm n_c}{2},\tag{36}$$

and the linearized equilibrium density profiles,

$$n_{\pm}(x) = \bar{n}_{\pm} [1 \pm \langle\psi(x)\rangle_1 \mp \psi(x)],\tag{37}$$

where the notation  $\langle \dots \rangle_1$  emphasizes the fact that the self-consistent averaged densities (36) were obtained within a *linearized* approximation. Henceforth we will omit the subscript ‘1’ in order to simplify the notation.

We should remark that the profile independence of the self-consistent linearized averaged densities given by (36) can only be verified *after* the minimization procedure. When performing the functional minimization of the linearized functional  $\Omega_{\text{DH}}[n_{\pm}(x)]$ , one must take the profile dependence of the average expansion densities  $\langle n_{\pm}(x) \rangle$  into account, in addition to the charge-neutrality constraint (5). Although similar quadratic expansions about the zero-th order Donnan densities for the planar case were already proposed by Trizac and Hansen,<sup>29</sup> they focused their study on finite-size effects and did not investigate the consequences of the linearization in detail. Deserno and von Grünberg<sup>3</sup> considered the general  $d$ -dimensional problem in a fixed-gauge formulation, interpreting these self-consistent linearized averaged densities in terms of an optimal linearization point,  $\bar{n}_{\pm} = n_{\text{b}} e^{\mp \psi_{\text{opt}}}$ .

The linearized expansion densities (36), which correspond to the state-independent zero-th order Donnan densities, represent the infinite-temperature ( $\ell_B = 0$ ) limit of the gauge-invariant forms of the equilibrium density profiles (11) and *do not coincide* with the exact nonlinear averages,

$$\langle n_{\pm}(x) \rangle = \frac{\sqrt{n_{\text{c}}^2 + (2n_{\text{b}})^2 \alpha_{+} \alpha_{-}} \pm n_{\text{c}}}{2} = \frac{\sqrt{n_{\text{c}}^2 + (2n_{\text{b}})^2 e^{\langle \delta_2(x) \rangle} + \mathcal{O}[\langle \delta_3(x) \rangle]} \pm n_{\text{c}}}{2}, \quad (38)$$

because of the nonvanishing quadratic and higher-order ( $\nu \geq 2$ ) contributions of the electrostatic-potential deviations,

$$\delta_{\nu}(x) \equiv [\langle \psi \rangle - \psi(x)]^{\nu}. \quad (39)$$

In Appendix A we compare the uniform self-consistent linearized expansion densities (36) with the exact nonlinear averages (38). Justification of the neglect of the quadratic and higher-order contributions under linearized theory, which was done for the spherical case — but is trivially generalized for the planar case — is found in Appendix F of Ref. [1]. However, we should mention that — although *internal* (within the semi-grand-canonical ensemble) self-consistency under linearization is achieved by using the uniform expansion densities (36) — *global* self-consistency (preserving the exact nature of the Legendre transformation between the semi-grand-canonical and canonical ensembles) requires also the inclusion of the quadratic contribution of the averages (38), as discussed in detail in Appendix G of Ref. [1]. The linearized equations including these quadratic contributions to the expansion densities are presented in Appendix D, where it is shown that their inclusion do not improve the agreement between the linearized and the full nonlinear equations.

Inserting the linearized equilibrium density profiles (37) into the Poisson equation (2) yields the Debye-Hückel-like (DH) equation,<sup>30</sup>

$$\frac{d^2 \psi(x)}{dx^2} = \kappa^2 [\psi(x) - \langle \psi(x) \rangle - \eta] + \frac{2}{\Lambda} [\delta(x+L) + \delta(x-L)], \quad (40)$$

where the parameter

$$\eta \equiv \frac{\bar{n}_{+} - \bar{n}_{-}}{\bar{n}_{+} + \bar{n}_{-}} = \frac{n_{\text{c}}}{\sqrt{n_{\text{c}}^2 + (2n_{\text{b}})^2}}, \quad (41)$$

measures the relative importance of the counterions to the ionic strength in the interplane region  $|x| \leq L$ ,

$$I \equiv \frac{1}{2} (\bar{n}_{+} + \bar{n}_{-}) = \frac{1}{2} \sqrt{n_{\text{c}}^2 + (2n_{\text{b}})^2} = \frac{n_{\text{c}}}{2\eta} = \frac{n_{\text{b}}}{\sqrt{1 - \eta^2}}. \quad (42)$$

The (effective) Debye screening length in the interplane region  $\kappa^{-1}$  satisfies

$$\kappa^2 = 8\pi \ell_B I = \frac{\kappa_{\text{b}}^2}{\sqrt{1 - \eta^2}} > \kappa_{\text{b}}^2, \quad (43)$$

showing that screening is enhanced compared to the salt reservoir.

The gauge-invariant linearized electrostatic potential satisfying the DH-like equation (40) subject to the boundary conditions (13) can be readily obtained,

$$\psi(x) = \langle \psi(x) \rangle + \eta \left( 1 - \kappa L \frac{\cosh \kappa x}{\sinh \kappa L} \right), \quad (44)$$

where the average electrostatic potential for *an arbitrary* electrostatic surface potential  $\psi_L$  is given by

$$\langle \psi(x) \rangle = \psi_L + \eta \kappa L \mathcal{L}(\kappa L), \quad (45)$$

in terms of the Langevin function,

$$\mathcal{L}(x) \equiv \coth x - \frac{1}{x}. \quad (46)$$

The linearized semi-grand-canonical potential,  $\Omega_{\text{DH}} \equiv \Omega_{\text{DH}}[n_{\pm}(x)]_{\text{equil}}$ , is obtained by inserting the equilibrium density profiles (37) — recalling that the self-consistent linearized averages,  $\langle n_{\pm}(x) \rangle = \bar{n}_{\pm}$ , are given by Eq. (36) — and the DH-like solution (44) into the linearized semi-grand-canonical functional  $\Omega_{\text{DH}}[n_{\pm}(x)]$ , Eq. (35). After performing the integrations, we may cast the linearized semi-grand-canonical potential (per unit area) in the form

$$\frac{\beta\Omega_{\text{DH}}}{A} = \sigma \left( \operatorname{arctanh} \eta - \frac{1}{\eta} \right) + \frac{1}{2} \eta \sigma \kappa L \mathcal{L}(\kappa L), \quad (47)$$

which yields the dimensionless excess linearized semi-grand-canonical potential per unit area,

$$\omega_{\text{DH}}(\lambda, l) \equiv \frac{\kappa_{\text{b}}}{2n_{\text{b}}} \left[ \frac{\beta\Omega_{\text{DH}}(\Lambda, L)}{A} + 2n_{\text{b}}L \right] = \frac{2}{\lambda} \left[ \operatorname{arctanh} \eta - \frac{1}{\eta} + \frac{1}{2} \eta \kappa l \mathcal{L}(\kappa l) \right] + l, \quad (48)$$

written in terms of the dimensionless lengths

$$k^{-1} \equiv \kappa_{\text{b}} \kappa^{-1}, \quad l \equiv \kappa_{\text{b}} L, \quad \lambda \equiv \kappa_{\text{b}} \Lambda. \quad (49)$$

With these definitions we obtain the linearized self-energy  $\omega_{\text{DH}}(\lambda, l \rightarrow \infty) = 2/\lambda^2$  and

$$\eta = \eta(\lambda, l) = \frac{1}{\sqrt{1 + (\lambda l/2)^2}}, \quad k^2 = k^2(\lambda, l) = \sqrt{1 + [2/(\lambda l)]^2} = \frac{1}{\sqrt{1 - \eta^2(\lambda, l)}}. \quad (50)$$

The dimensionless linearized osmotic-pressure difference is then given by

$$\begin{aligned} \Pi_{\text{DH}} &\equiv \frac{\beta \Delta P_{\text{DH}}}{2n_{\text{b}}} = -\frac{1}{2n_{\text{b}}} \frac{d}{dL} \left[ \frac{\beta\Omega_{\text{DH}}(\Lambda, L)}{A} + 2n_{\text{b}}L \right]_{\sigma, \ell_{\text{B}}, \mu_{\pm}} = -\frac{d\omega_{\text{DH}}(\lambda, l)}{dl} \\ &= k^2 \left\{ 1 + \eta^2 \left( 1 - \frac{3}{4} \eta^2 \right) \kappa l \mathcal{L}(\kappa l) + \frac{1}{2} \eta^2 \left( 1 - \frac{1}{2} \eta^2 \right) (\kappa l)^2 [\mathcal{L}^2(\kappa l) - 1] \right\} - 1, \end{aligned} \quad (51)$$

where we have made use of the total derivative,

$$\frac{d}{dl} = \frac{\partial}{\partial l} + \frac{d\eta}{dl} \frac{\partial}{\partial \eta} + \frac{dk}{dl} \frac{\partial}{\partial k} = \frac{\partial}{\partial l} - \frac{\eta}{l} (1 - \eta^2) \frac{\partial}{\partial \eta} - \frac{k\eta^2}{2l} \frac{\partial}{\partial k}, \quad (52)$$

and the derivative of the Langevin function,

$$\mathcal{L}'(x) = 1 - \frac{2}{x} \mathcal{L}(x) - \mathcal{L}^2(x). \quad (53)$$

Alternatively, the same expression for the linearized osmotic-pressure difference may be obtained by performing a quadratic expansion of the gauge-invariant form of the nonlinear PB osmotic pressure (34) — similarly as obtained for the spherical case in Appendix E of Ref. [1],

$$\Pi_{\text{DH}} = k^2 \left[ 1 + \eta \delta_1(0) + \frac{1}{2} \delta_2(0) - \frac{1}{2} \eta^2 \langle \delta_2(x) \rangle \right] - 1, \quad (54)$$

where the  $\nu$ -th order electrostatic-potential differences (39) read

$$\delta_{\nu}(x) = \eta^{\nu} \left( \kappa L \frac{\cosh \kappa x}{\sinh \kappa L} - 1 \right)^{\nu}. \quad (55)$$

In the next section we will investigate the properties of the linearized osmotic-pressure difference defined by Eqs. (51) or (54) and compare it with its exact nonlinear counterpart (33).

## 4 Comparison of the exact nonlinear and the linearized equations of state

As already pointed out in the literature,<sup>2,3</sup> the linearized osmotic-pressure difference  $\Pi_{\text{DH}}$  defined by Eqs. (51) or (54) yields artifacts in the low-temperature, large-separation or high-surface charge limits. In contradiction to the exact nonlinear result (33), which predicts that the osmotic-pressure difference is always positive,  $\Pi > 0$ , the linearized version  $\Pi_{\text{DH}}$  becomes negative in the above mentioned limits. In an attempt to define the osmotic pressure in a linearized framework, Deserno and von Grünberg<sup>2</sup> introduced an additional (alternative) definition,  $\Pi_1$ , cf. Eq. (43) of Ref. [3], that does not have the shortcoming of displaying any instabilities. On the other hand, we will show later that their partially unstable osmotic-pressure definition, cf. Eq. (44) of Ref. [3], coincides with the linearized version (51) obtained in the previous section,  $\Pi_2 \equiv \Pi_{\text{DH}}$ . Their general formulas, for the planar case ( $d = 1$ ), need to be taken in the formal limit of vanishing volume fraction,  $\phi \equiv a/l \rightarrow 0$  — with  $a > 0$  being some arbitrary (reduced) length — which yields

$$\begin{aligned} \Pi_1 &\equiv \frac{\beta P_1}{2n_b} - 1 = \cosh \bar{\psi}_{\text{opt}} - \frac{\sinh^2 \bar{\psi}_{\text{opt}}}{2 \cosh \bar{\psi}_{\text{opt}}} \left[ 1 - \lim_{a \rightarrow 0} \left( \frac{1 - a/l}{\mathcal{D} \sqrt{a/l}} \right)^2 \right] - 1 \\ &= \frac{1}{2k^2} (k^2 - 1)^2 + \frac{1}{2} \left( \frac{\eta k^2 l}{\sinh kl} \right)^2 \geq 0, \end{aligned} \quad (56)$$

$$\begin{aligned} \Pi_2 &\equiv \frac{\beta P_2}{2n_b} - 1 = \frac{\beta P_1}{2n_b} - \frac{\sinh^4 \bar{\psi}_{\text{opt}}}{2 \cosh^3 \bar{\psi}_{\text{opt}}} \lim_{a \rightarrow 0} \left\{ \frac{1 - a/l}{2a/l} \left[ \frac{1}{\mathcal{D}^2} + ka \frac{\mathcal{E}}{\mathcal{D}} + k^2 a^2 \left( 1 - \frac{\mathcal{E}^2}{\mathcal{D}^2} \right) \right] - 1 \right\} \\ &= \Pi_1 - \frac{1}{4} k^2 \eta^4 \left( \frac{k^2 l^2}{\sinh^2 kl} + kl \coth kl - 2 \right), \end{aligned} \quad (57)$$

$$\mathcal{D} = K_{1/2}(ka) I_{1/2}(kl) - K_{1/2}(kl) I_{1/2}(ka), \quad (58)$$

$$\mathcal{E} = K_{-1/2}(ka) I_{1/2}(kl) + K_{1/2}(kl) I_{-1/2}(ka), \quad (59)$$

where  $\{I_\nu, K_\nu\}$  are the modified Bessel functions<sup>19</sup> of the first and the second kind, respectively, and  $\bar{\psi}_{\text{opt}}$  is the optimal linearization point, satisfying the relations

$$\tanh \bar{\psi}_{\text{opt}} = -\eta, \quad \cosh \bar{\psi}_{\text{opt}} = \left( \frac{\kappa}{\kappa_b} \right)^2 = k^2, \quad \sinh \bar{\psi}_{\text{opt}} = -\frac{n_c}{2n_b} = -\frac{2}{\lambda l}. \quad (60)$$

In accordance with Eqs. (23) and (26) of Ref. [3], the two osmotic-pressure definitions can be recast in a simpler formal form,

$$\Pi_1 = k^2 \left[ 1 + \eta \delta_1(0) + \frac{1}{2} \delta_2(0) \right] - 1, \quad (61)$$

$$\Pi_2 = k^2 \left[ 1 + \eta \delta_1(0) + \frac{1}{2} \delta_2(0) - \frac{1}{2} \eta^2 \langle \delta_2(x) \rangle \right] - 1, \quad (62)$$

from which one can see that the second osmotic-pressure definition coincides with the linearized osmotic-pressure difference (51) obtained in the last section,  $\Pi_2 \equiv \Pi_{\text{DH}}$ , while the first one  $\Pi_1$  differs from Eq. (54) by an omitted quadratic term. Analogously to the spherical case,<sup>1</sup> the term that distinguishes the two distinct osmotic-pressure definitions originates from the volume dependence of the optimal linearization point  $\bar{\psi}_{\text{opt}}$ , as pointed out by Deserno and von Grünberg.<sup>3</sup>

From its asymptotic expansions to be given next and its formal expression (61), we see that  $\Pi_1$ , although *fully thermodynamically stable* — related to its positiveness, cf. Eq. (56) — is *inconsistent* with a quadratic expansion of the gauge-invariant nonlinear PB pressure (34), because of the omitted last quadratic term of (54). Furthermore, we will show next that the *consistent* — although *partially unstable* — linearized osmotic-pressure difference  $\Pi_2$  presents indeed a better agreement with the nonlinear osmotic pressure  $\Pi$  in the weak-coupling and counterionic ideal-gas limits, when the underlying assumptions of the linearization are fulfilled. Therefore, although the alternative  $\Pi_1$  displays the *fortuitous* advantage of preserving the

positiveness of the exact nonlinear pressure  $\Pi$ , its derivation has no justification in our approach based on the minimization of the linearized semi-grand-canonical functional  $\Omega_{\text{DH}}[n_{\pm}(x)]$ . Moreover, the partially unstable  $\Pi_2$  corresponds indeed to the negative *total derivative* of the linearized semi-grand-canonical potential  $\omega_{\text{DH}}$  with respect to the planes separation  $l$ , which we thus believe to be the consistent and correct definition of the osmotic pressure.

Let us now perform an explicit comparison between asymptotic expressions of  $\Pi$ , the nonlinear osmotic pressure<sup>35</sup> — obtained in Appendix B — and of the two corresponding linearized versions,  $\Pi_1$  and  $\Pi_2$ , for the distinct regimes listed below.

- Weak-coupling or zero-th order Donnan ( $\ell_B \rightarrow 0$ ) limit:  $l \rightarrow 0$ ,  $\lambda \rightarrow \infty$ , but finite product  $\lambda l$

$$\begin{aligned} \Pi = k^2 \left[ 1 - \frac{\eta^2}{6} k^2 l^2 - \frac{\eta^2}{90} (\eta^2 - 3) k^4 l^4 + \frac{\eta^2}{945} (3\eta^2 - 5) k^6 l^6 - \frac{\eta^2}{113400} (7\eta^6 + 18\eta^4 + 51\eta^2 - 84) k^8 l^8 \right. \\ \left. + \mathcal{O}(k^{10} l^{10}) \right] - 1, \end{aligned} \quad (63)$$

$$\Pi_1 = k^2 \left[ 1 - \frac{\eta^2}{6} k^2 l^2 + \frac{\eta^2}{30} k^4 l^4 - \frac{\eta^2}{189} k^6 l^6 + \frac{\eta^2}{1350} k^8 l^8 + \mathcal{O}(k^{10} l^{10}) \right] - 1, \quad (64)$$

$$\Pi_2 = k^2 \left[ 1 - \frac{\eta^2}{6} k^2 l^2 - \frac{\eta^2}{90} (\eta^2 - 3) k^4 l^4 + \frac{\eta^2}{945} (2\eta^2 - 5) k^6 l^6 - \frac{\eta^2}{9450} (3\eta^2 - 7) k^8 l^8 + \mathcal{O}(k^{10} l^{10}) \right] - 1, \quad (65)$$

- Counterionic ideal-gas limit:  $l \rightarrow 0$  and finite  $\lambda$

$$\Pi = \frac{2}{\lambda l} \left\{ 1 - \frac{l}{3\lambda} + \left( \frac{4}{45} + \frac{\lambda^4}{8} \right) \left( \frac{l}{\lambda} \right)^2 - \frac{16}{945} \left( \frac{l}{\lambda} \right)^3 + \mathcal{O} \left[ (l/\lambda)^4 \right] \right\} - 1, \quad (66)$$

$$\Pi_1 = \frac{2}{\lambda l} \left\{ 1 - \frac{l}{3\lambda} + \left( \frac{2}{15} + \frac{\lambda^4}{8} \right) \left( \frac{l}{\lambda} \right)^2 - \frac{8}{189} \left( \frac{l}{\lambda} \right)^3 + \mathcal{O} \left[ (l/\lambda)^4 \right] \right\} - 1, \quad (67)$$

$$\Pi_2 = \frac{2}{\lambda l} \left\{ 1 - \frac{l}{3\lambda} + \left( \frac{4}{45} + \frac{\lambda^4}{8} \right) \left( \frac{l}{\lambda} \right)^2 - \frac{8}{315} \left( \frac{l}{\lambda} \right)^3 + \mathcal{O} \left[ (l/\lambda)^4 \right] \right\} - 1, \quad (68)$$

- Gouy-Chapman or high-surface charge limit:  $l \rightarrow 0$  and  $\lambda/l \rightarrow 0$

$$\Pi = \frac{1}{2} \left( \frac{\pi}{l} \right)^2 \left\{ 1 - \frac{2\lambda}{l} + \mathcal{O} \left[ (\lambda/l)^3 \right] \right\} - 1 + \mathcal{O}(l^2), \quad (69)$$

$$\Pi_1 = \frac{2}{\lambda^2 \sinh^2 \sqrt{2l/\lambda}} + \frac{1}{\lambda l} - \frac{l^2 \sqrt{2l/\lambda} \coth \sqrt{2l/\lambda}}{4 \sinh^2 \sqrt{2l/\lambda}} - 1 + \mathcal{O}(\sqrt{\lambda/l}), \quad (70)$$

$$\Pi_2 = \frac{1}{\lambda^2 \sinh^2 \sqrt{2l/\lambda}} - \frac{\coth \sqrt{2l/\lambda}}{\lambda^2 \sqrt{2l/\lambda}} + \frac{2}{\lambda l} + \mathcal{O}(\sqrt{l/\lambda}), \quad (71)$$

- Large-separation limit:  $l \rightarrow \infty$  and finite  $\lambda$

$$\Pi = \frac{32e^{-2l}}{(\lambda + \sqrt{1 + \lambda^2})^2} \left\{ 1 - 8 \left[ l - 1 + \frac{\lambda(1 - \lambda^2)}{\sqrt{1 + \lambda^2}} \right] \frac{e^{-2l}}{(\lambda + \sqrt{1 + \lambda^2})^2} + \mathcal{O}(l^2 e^{-4l}) \right\}, \quad (72)$$

$$\begin{aligned} \Pi_1 = \frac{1}{\sinh^2 l} \left[ \frac{2}{\lambda^2} - \frac{4 \coth l}{\lambda^4 l} - \frac{2(1 - 3 \coth^2 l)}{\lambda^6 l^2} + \frac{2(8 + 9\lambda^2 - 12 \coth^2 l) \coth l}{3\lambda^8 l^3} \right] + \frac{2[1 + \mathcal{O}(e^{-2l})]}{\lambda^4 l^4} \\ + \mathcal{O}(l^{-5}), \end{aligned} \quad (73)$$

$$\Pi_2 = \frac{1}{\sinh^2 l} \left[ \frac{2}{\lambda^2} - \frac{4 \coth l}{\lambda^4 l} - \frac{2(1 + 2\lambda^2 - 3 \coth^2 l)}{\lambda^6 l^2} \right] - \frac{4[1 + \mathcal{O}(e^{-2l})]}{\lambda^4 l^3} + \mathcal{O}(l^{-4}). \quad (74)$$

Looking at Eqs. (71) and (74) one may see why the linearized osmotic-pressure difference  $\Pi_2$  becomes negative at the Gouy-Chapman and large-separation limits. In the Gouy-Chapman limit the leading term is given by the  $\mathcal{O}(\lambda^{-3/2})$ , which is negative and overcomes the exponentially decaying  $\mathcal{O}(\lambda^{-2})$  term. The leading term of the large-separation limit is given by the  $\mathcal{O}(l^{-3})$  contribution, which is negative and overcomes the three exponentially decaying lowest-order terms. In the full nonlinear solution, however, all algebraically decaying terms cancel in a nontrivial way, and eventually only an exponentially (positive) decaying behavior is predicted. Note that both linearized versions,  $\Pi_1$  and  $\Pi_2$ , show asymptotic behaviours that disagree strongly from the nonlinear osmotic-pressure difference  $\Pi$ . This clearly indicates that both linearized osmotic-pressure definitions are meaningless in these limits and so is the positiveness of  $\Pi_1$ .

We see that in the weak-coupling limit the self-consistent linearized osmotic pressure  $\Pi_2$  and its nonlinear counterpart  $\Pi$  agree up to the  $\mathcal{O}(l^4)$  terms, confirming the validity of the linearization when its underlying assumptions are fulfilled. The same occurs for the counterionic ideal-gas limit up to the  $\mathcal{O}(l)$  terms. In both cases the fully stable  $\Pi_1$  has a worse agreement, one order lower than the partially unstable  $\Pi_2$ . However, in the large-separation limit, the two linearized and the nonlinear expressions disagree even qualitatively: the linearized asymptotics is algebraic (negative for  $\Pi_2$ , positive for  $\Pi_1$ ), whereas the nonlinear is exponential (and positive). On the other hand, although in the Gouy-Chapman limit all asymptotics are algebraic, in the linearized case the power-law is  $\propto -l^{-1/2}$  for  $\Pi_2$  and  $\propto l^{-1}$  for  $\Pi_1$ , both in disagreement with the nonlinear asymptotics  $\propto l^{-2}$ . The failure of the linearization scheme should not be at all surprising, because it is supposed to be valid in the weak-coupling ( $\ell_B \rightarrow 0$ ) and counterionic ideal-gas limit, but not in the opposite, large-separation ( $l \rightarrow \infty$ ) or high-surface charge, Gouy-Chapman, ( $\lambda \rightarrow 0$ ) limits. Therefore, any results obtained in a linearized framework outside the weak-coupling and the counterionic ideal-gas limits should be taken with caution. See also our comments in the concluding remarks of the preceding paper<sup>1</sup> on the gas-liquid-like phase separation in dilute deionized aqueous suspensions of charged colloidal particles.

In order to show the accuracy of the self-consistent linearized osmotic-pressure difference  $\Pi_{\text{DH}}$ , Eq. (51), and the region where the linearization scheme breaks down, we plotted in Figures 1 and 2 the loci of constant errors between the exact nonlinear PB osmotic-pressure difference and the corresponding linearized version, measured by the logarithmic deviations

$$\delta\Pi_{\text{DH}} \equiv |\ln \Pi_{\text{DH}}(\lambda, l) - \ln \Pi(\lambda, l)|. \quad (75)$$

We have chosen a logarithmic measure for the deviations because  $\Pi$  varies in a range of several orders of magnitude. For small deviations, this definition leads to the relative errors,

$$\delta\Pi_{\text{DH}} \approx \left| \frac{\Pi_{\text{DH}}(\lambda, l) - \Pi(\lambda, l)}{\Pi(\lambda, l)} \right|. \quad (76)$$

Analogously, we may define the logarithmic deviation from PB of the linearized semi-grand-canonical potential,

$$\delta\omega_{\text{DH}} \equiv |\ln [\omega_{\text{DH}}(\lambda, l) - \omega(\lambda, \infty)] - \ln [\omega(\lambda, l) - \omega(\lambda, \infty)]|, \quad (77)$$

which is always smaller than  $\delta\Pi_{\text{DH}}$  (not shown). Therefore the linearized semi-grand-canonical potential, Eq. (48), and the linearized osmotic-pressure difference, Eq. (51), describe well the corresponding nonlinear equations in the limit  $\lambda/l \gg 1$  and  $l \ll 1$ . Because the nonlinear theory always predicts repulsion, the attractive osmotic-pressure region — shown in gray in Figures 1 and 2 — is clearly an artifact of the linearization. When plotted on the  $\Lambda/L \times (\kappa_b L)^{-1}$  plane, the  $\Pi_{\text{DH}} = 0$  line reaches at  $\kappa_b L \rightarrow 0$  the asymptotic value  $\xi_0 = \Lambda/L = 0.123863965 \dots$ , which is given by the solution of the transcendental equation

$$2\xi_0 + \sqrt{\frac{\xi_0}{2}} \mathcal{L} \left( \sqrt{\frac{2}{\xi_0}} \right) + \mathcal{L}^2 \left( \sqrt{\frac{2}{\xi_0}} \right) = 1. \quad (78)$$

To obtain the full nonlinear PB osmotic-pressure difference  $\Pi$ , one needs to numerically solve the transcendental equation (22) involving elliptic functions or elliptic integrals. Although the asymptotic expansions of the nonlinear  $\Pi$  represented by Eqs. (63), (66), (69) and (72) allow an explicit analytical comparison in the distinct regimes with their linearized versions, they are not very useful for numerical evaluation. In Appendix C we derive extended expansions of the nonlinear PB semi-grand-canonical potential  $\omega$ , Eq. (30), and

of the PB osmotic-pressure difference  $\Pi$ , Eq. (33), that involve only elementary functions and are suitable for numerical implementation. These extend the numerical accuracy of the above mentioned asymptotic expansions of the full nonlinear  $\Pi$  and are complementary to the linearized equations,  $\omega_{\text{DH}}$ , Eq. (48), and  $\Pi_{\text{DH}}$ , Eq. (51), providing an excellent approximation in the regions where the linearization scheme breaks down. In Figures 1 and 2 we also present their corresponding logarithmic deviations from the exact PB result, which, similarly to (75), are defined by

$$\delta\Pi_{\text{GC}} \equiv |\ln \Pi_{\text{GC}}(\lambda, l) - \ln \Pi(\lambda, l)|, \quad (79)$$

$$\delta\Pi_{\text{LS}} \equiv |\ln \Pi_{\text{LS}}(\lambda, l) - \ln \Pi(\lambda, l)|, \quad (80)$$

where  $\Pi_{\text{GC}}$  and  $\Pi_{\text{LS}}$ , given explicitly in Appendix C, are the osmotic-pressure differences in the extended Gouy-Chapman and large-separation limits, respectively.

## 5 Concluding remarks

The classical problem of two infinite uniformly charged planes in electrochemical equilibrium with an infinite salt-reservoir is exactly solved at the mean-field nonlinear level, as well as by a linearization scheme consistent with quadratic expansions of the nonlinear semi-grand-canonical functional. By using gauge-invariant forms of the electrostatic potential, we have shown that the linearized osmotic pressure corresponds to a quadratic expansion of the corresponding nonlinear version.

As already pointed out in the literature,<sup>3</sup> it is shown that the self-consistent linearized osmotic pressure leads to artifacts in the large-separation and the Gouy-Chapman (high-surface charge) limits, predicting there negative osmotic-pressure differences. Although it is possible to define an alternative linearized osmotic pressure that it is fully stable based on the *partial derivative* of the linearized semi-grand-canonical potential with respect to the separation distance,<sup>3</sup> its stability is shown to be a fortuitous result. In fact explicit comparison of the exact nonlinear osmotic pressure and the two linearized versions shows that the linearized self-consistent osmotic pressure, though partially unstable, presents a better agreement with the PB results in the weak-coupling and counterion ideal-gas limits, where the linearization can be applied. However, not surprisingly, in the region where the linearization breaks down none of both proposed linearized osmotic pressures give quantitatively correct results.

To avoid confusion we should stress at this point the exactness of the PB nonlinear solution at the mean-field level and discuss its range of validity and limitations. It is known from numerical simulations of the Primitive Model<sup>37</sup> (PM) in the planar geometry that sufficiently close and highly charged planes in the presence of neutralizing counterions attract each other,<sup>38</sup> even though for realistic charge densities and monovalent ions this is not observed at room temperature. In this case the attraction is prevented by steric repulsions at the small separations at which it would be observed neglecting the finite ionic size. Because the mean-field PB approximation always predicts repulsion, theoretical validation for this attraction (observed in fact at room temperature only for multivalent ions) has to be given beyond the PB level, e.g., by bulk counterion correlations,<sup>39,40</sup> integral-equations theories,<sup>41,42</sup> charge-correlation-induced attractions,<sup>43,44</sup> charge-fluctuation-induced attractions,<sup>45,46,47</sup> electrolytic depletion-induced attractions,<sup>48</sup> discrete solvent-mediated attractions,<sup>49</sup> field-theory methods<sup>50</sup> etc — see also Refs. [51, 52, 53, 54, 55, 56, 57, 58, 59, 60] for mechanisms of attraction between like-charged rods. On the other hand, in the strong-coupling limit the linearization of the WS-cell mean-field PB equation, as discussed in this work, *does predict* attraction. However, here the mechanism of attraction is related to mathematical artifacts of the linearization itself and does not correspond to a real physical effect. The fact that this prediction is in agreement with the theories beyond the mean-field level is purely *accidental* and is intrinsically connected with the *inadequacy* (meaning incorrect application) of the PB mean-field approach at the same limit. In other words, a *qualitatively* correct result (in this example, attraction) may be deceptively anticipated in the strong-coupling limit because of the simultaneous application of two inadequate approximations, namely, the mean-field PB equation and its subsequent linearization.

## Acknowledgments

M. N. T. would like to thank the Alexander von Humboldt-Stiftung for financial support.

## A Exact nonlinear averaged densities

In this Appendix we will compare the uniform expansion densities about which the linearization is performed — the state-independent zero-th order Donnan densities — with the exact nonlinear PB averages.

By using the definite integrals

$$\int_{\varphi_L}^{\varphi_0} \frac{d\varphi \sinh \varphi}{\sqrt{2 \cosh \varphi - 2 \cosh \varphi_0}} = -\sqrt{2 \cosh \varphi_L - 2 \cosh \varphi_0}, \quad (\text{A1})$$

$$\begin{aligned} \int_{\varphi_L}^{\varphi_0} \frac{d\varphi \cosh \varphi}{\sqrt{2 \cosh \varphi - 2 \cosh \varphi_0}} &= \frac{\cosh \varphi_0}{\cosh \frac{\varphi_0}{2}} F \left( \arccos \left[ \sinh \frac{\varphi_0}{2} / \sinh \frac{\varphi_L}{2} \right] \middle| 1 / \cosh^2 \frac{\varphi_0}{2} \right) \\ &\quad - 2 \cosh \frac{\varphi_0}{2} E \left( \arccos \left[ \sinh \frac{\varphi_0}{2} / \sinh \frac{\varphi_L}{2} \right] \middle| 1 / \cosh^2 \frac{\varphi_0}{2} \right) \\ &\quad - \coth \frac{\varphi_L}{2} \sqrt{2 \cosh \varphi_L - 2 \cosh \varphi_0}, \end{aligned} \quad (\text{A2})$$

it is possible to obtain the exact nonlinear PB averaged densities,

$$\begin{aligned} \frac{\langle n_{\pm}(x) \rangle}{n_b} &= \langle e^{\mp \varphi(x)} \rangle = \sqrt{\left( \frac{2}{\lambda l} \right)^2 + \langle e^{\varphi(x)} \rangle \langle e^{-\varphi(x)} \rangle} \pm \frac{2}{\lambda l} \\ &= 1 + 2t \pm \frac{2}{\lambda l} - \frac{2}{l} \sqrt{1+t} E \left[ \arctan \left( \frac{1}{\lambda \sqrt{t}} \right) \middle| \frac{1}{1+t} \right] + \frac{2}{\lambda l} \sqrt{\frac{1+\lambda^2(1+t)}{1+\lambda^2 t}}. \end{aligned} \quad (\text{A3})$$

In Figure 3 we compare them with the uniform densities about which the linearization is performed, the state-independent zero-th order Donnan densities (36),

$$\frac{\bar{n}_{\pm}}{n_b} = \sqrt{\left( \frac{2}{\lambda l} \right)^2 + 1} \pm \frac{2}{\lambda l}, \quad (\text{A4})$$

by looking at their logarithmic deviations from the corresponding exact PB averages,

$$\delta \bar{n}_{\pm} \equiv \ln \langle n_{\pm}(x) \rangle - \ln \bar{n}_{\pm}. \quad (\text{A5})$$

## B Asymptotic expansions of the nonlinear solution

In this Appendix we obtain the asymptotic expansions of the nonlinear osmotic-pressure difference  $\Pi$ . We have made extensive use of Refs. [18, 19, 20, 21] throughout this Appendix.

### B.1 Weak-coupling limit

To obtain the weak-coupling ( $\ell_B \rightarrow 0$ ) limit, first note that the product  $\lambda l = 2/(\eta k^2)$  does not depend on  $\ell_B$ . Therefore we multiply both sides of the eigenvalue equation by  $l$ ,

$$\lambda l \sqrt{t} = \frac{2\sqrt{t}}{\eta k^2} = l \operatorname{cs} \left( l \sqrt{1+t} \middle| \frac{1}{1+t} \right), \quad (\text{B1})$$

and expand them in powers of  $l$ , assuming that  $t = \sum_{k=0}^{\infty} a_{2k} l^{2k}$ . It is then possible to obtain the coefficients  $\{a_{2k}\}$  of the expansion recursively, leading to Eq. (63).

### B.2 Counterionic ideal-gas limit

To obtain the counterion-dominated ideal-gas limit ( $l \rightarrow 0$  and finite  $\lambda$ ), we write

$$\lambda \sqrt{t} = \operatorname{cs} \left( l \sqrt{1+t} \middle| \frac{1}{1+t} \right), \quad (\text{B2})$$

and expand the right-hand side in powers of  $l$ , assuming that  $t = \sum_{k=-1}^{\infty} a_k l^k$ . It is then possible to obtain the coefficients  $\{a_k\}$  of the expansion recursively, leading to Eq. (66).

### B.3 Gouy-Chapman limit

To obtain the Gouy-Chapman (high-surface charge) limit ( $\lambda \rightarrow 0$ ), note that

$$l\sqrt{1+t} = F \left[ \frac{\pi}{2} - \arctan(\lambda\sqrt{t}) \middle| \frac{1}{1+t} \right] = K \left( \frac{1}{1+t} \right) - \lambda\sqrt{1+t} + \mathcal{O}(\lambda^3 t), \quad (\text{B3})$$

leading to

$$l \left[ 1 + \frac{\lambda}{l} + \mathcal{O}(\lambda^3 t/l) \right] = \frac{1}{\sqrt{1+t}} K \left( \frac{1}{1+t} \right). \quad (\text{B4})$$

If we additionally assume that  $l \rightarrow 0$ , with  $\lambda/l \rightarrow 0$ , and with the help of the expansion of the complete elliptic integral  $K(m)$  about  $m = 0$ ,

$$K(m) = \frac{\pi}{2} \left[ 1 + \frac{m}{4} + \mathcal{O}(m^2) \right], \quad (\text{B5})$$

we are lead to the asymptotic solution,

$$t = \left( \frac{\pi}{2l} \right)^2 \left\{ 1 - \frac{2\lambda}{l} + \mathcal{O} \left[ (\lambda/l)^3 \right] \right\} - \frac{1}{2} + \mathcal{O}(l^2), \quad (\text{B6})$$

which gives the asymptotic osmotic-pressure difference in the Gouy-Chapman limit, Eq. (69). Evaluation of higher-order terms of the leading contribution  $\mathcal{O}(l^{-2})$  of the expansion would give

$$t = \left( \frac{\pi}{2l} \right)^2 \left\{ 1 - \frac{2\lambda}{l} + 3 \left( \frac{\lambda}{l} \right)^2 + \left( \frac{\pi^2}{6} - 4 \right) \left( \frac{\lambda}{l} \right)^3 - 5 \left( \frac{\pi^2}{6} - 1 \right) \left( \frac{\lambda}{l} \right)^4 - \left( \frac{\pi^4}{40} - \frac{5\pi^2}{2} + 6 \right) \left( \frac{\lambda}{l} \right)^5 + \mathcal{O} \left[ (\lambda/l)^6 \right] \right\} - \frac{1}{2} + \mathcal{O}(l^2). \quad (\text{B7})$$

### B.4 Large-separation limit

To obtain the large-separation ( $l \rightarrow \infty$  and finite  $\lambda$ ) asymptotics, first note that

$$\begin{aligned} l\sqrt{1+t} &= F \left[ \operatorname{arccotg}(\lambda\sqrt{t}) \middle| \frac{1}{1+t} \right] = F \left[ \frac{\pi}{2} - \arctan(\lambda\sqrt{t}) \middle| \frac{1}{1+t} \right] \\ &= K \left( \frac{1}{1+t} \right) - F \left[ \arctan(\lambda\sqrt{1+t}) \middle| \frac{1}{1+t} \right] \\ &= K \left( \frac{1}{1+t} \right) - F(\arctan \lambda | 1) + \mathcal{O}(t) = K \left( \frac{1}{1+t} \right) - \ln(\lambda + \sqrt{1+\lambda^2}) + \mathcal{O}(t). \end{aligned} \quad (\text{B8})$$

Using the expansion of the complete elliptic integral  $K(m)$  about  $m = 1$ ,

$$K(m) = \ln 4 - \frac{1}{2} \ln(1-m) + \mathcal{O}(1-m), \quad (\text{B9})$$

we are led to the asymptotic solution

$$t = \frac{16e^{-2l}}{(\lambda + \sqrt{1+\lambda^2})^2} + \mathcal{O}(le^{-4l}), \quad (\text{B10})$$

which yields the leading term of the asymptotic osmotic-pressure difference in the large-separation limit, Eq. (72). By computing higher-order terms, it is possible to write an asymptotic power series,

$$t = \frac{16e^{-2l}}{(\lambda + \sqrt{1+\lambda^2})^2} \left[ 1 + \sum_{\nu=1}^{\infty} \frac{e^{-2\nu l} t_{\nu}(\lambda, l)}{(\lambda + \sqrt{1+\lambda^2})^{2\nu}} \right], \quad (\text{B11})$$

where the coefficients  $t_\nu(\lambda, l) = \mathcal{O}(l^\nu)$  of the three leading terms read

$$t_1(\lambda, l) = -8 \left[ l - 1 + \frac{\lambda(1 - \lambda^2)}{\sqrt{1 + \lambda^2}} \right], \quad (\text{B12})$$

$$t_2(\lambda, l) = 96l^2 - 152l \left[ 1 - \frac{24\lambda(1 - \lambda^2)}{19\sqrt{1 + \lambda^2}} \right] + \frac{4}{1 + \lambda^2} (11 + 35\lambda^2 - 48\lambda^4 + 24\lambda^6) - \frac{8\lambda}{(1 + \lambda^2)^{3/2}} (19 - 12\lambda^2 - 17\lambda^4 + 6\lambda^6), \quad (\text{B13})$$

$$t_3(\lambda, l) = -\frac{4096l^3}{3} + 4096l^2 \left[ \frac{11}{16} - \frac{\lambda(1 - \lambda^2)}{\sqrt{1 + \lambda^2}} \right] + \frac{512\lambda l}{(1 + \lambda^2)^{3/2}} (11 - 6\lambda^2 - 10\lambda^4 + 3\lambda^6) - \frac{32l}{(1 + \lambda^2)^2} (47 + 222\lambda^2 - 81\lambda^4 - 128\lambda^6 + 128\lambda^8) - \frac{32\lambda}{(1 + \lambda^2)^{5/2}} (47 + 15\lambda^2 - 159\lambda^4 + 17\lambda^6 + 104\lambda^8 - 56\lambda^{10}) + \frac{64}{(1 + \lambda^2)^3} (3 + 53\lambda^2 - 39\lambda^4 - 77\lambda^6 + 72\lambda^8 + 36\lambda^{10} - 24\lambda^{12}). \quad (\text{B14})$$

Although this asymptotic series works pretty well for large separations ( $l \gg 1$ ), in the crossover region ( $l \approx 1$ ) it leads to oscillating pressures. In Appendix C we obtain extended expansions of the nonlinear equations in the large-separation limit that do not have this disadvantage in the crossover region.

## C Extended expansions of the nonlinear solution

In this Appendix we obtain extended expansions of the nonlinear semi-grand-canonical potential and of the nonlinear osmotic-pressure difference that are valid in the region where the linearization breaks down. Again, We have made extensive use of Refs. [18, 19, 20, 21] throughout this Appendix.

### C.1 Extended Gouy-Chapman limit

In the previous Appendix, both the counterionic ideal-gas (finite  $\lambda$ ) as well as the Gouy-Chapman ( $\lambda \rightarrow 0$ ) asymptotics were obtained in the small-separation ( $l \rightarrow 0$ ) limit. In fact, for any ratio  $\xi = \lambda/l$  the summation over the  $\lambda/l$  series for the leading terms up to  $\mathcal{O}(l^2)$  may be performed exactly, yielding

$$t = \left(\frac{y}{l}\right)^2 - \frac{1}{2} + \frac{3(1 + \xi + \xi^2 y^2)(1 + \xi^2 y^2) + 2\xi^3 y^2}{32y^2(1 + \xi + \xi^2 y^2)(1 + \xi^2 y^2)} l^2 + \mathcal{O}(l^4), \quad (\text{C1})$$

where  $y = y(\xi)$  is the solution of the transcendental equation

$$\xi y \tan y = 1. \quad (\text{C2})$$

This general expression yields the leading term  $\mathcal{O}(l^{-2})$  of the counterionic ideal-gas (finite  $\lambda$ , when  $y \rightarrow \sqrt{l/\lambda} \rightarrow 0$ ) as well as the Gouy-Chapman (high-surface charge, when  $\lambda \rightarrow 0, y \rightarrow \pi/2$ ) asymptotics as special cases,

$$y^2 = \frac{l}{\lambda} \left\{ 1 - \frac{l}{3\lambda} + \frac{4}{45} \left(\frac{l}{\lambda}\right)^2 - \frac{16}{945} \left(\frac{l}{\lambda}\right)^3 + \frac{16}{14175} \left(\frac{l}{\lambda}\right)^4 + \frac{64}{93555} \left(\frac{l}{\lambda}\right)^5 + \mathcal{O}\left[\left(\frac{l}{\lambda}\right)^6\right] \right\} = \left(\frac{\pi}{2}\right)^2 \left\{ 1 - \frac{2\lambda}{l} + 3 \left(\frac{\lambda}{l}\right)^2 + \left(\frac{\pi^2}{6} - 4\right) \left(\frac{\lambda}{l}\right)^3 - 5 \left(\frac{\pi^2}{6} - 1\right) \left(\frac{\lambda}{l}\right)^4 - \left(\frac{\pi^4}{40} - \frac{5\pi^2}{2} + 6\right) \left(\frac{\lambda}{l}\right)^5 + \mathcal{O}\left[\left(\frac{\lambda}{l}\right)^6\right] \right\}. \quad (\text{C3})$$

The excess semi-grand-canonical potential  $\omega$  may be obtained by integration of the osmotic-pressure difference  $2t$ , leading to

$$\omega(\lambda, l) = \frac{2y^2}{l} - \frac{4}{\lambda} \left[ 1 + \ln \left( \frac{\lambda}{2} \sin y \right) \right] + l - \frac{1}{2} \cot y \left( \sin^2 y + \frac{l}{\lambda} \right) \left( \frac{l}{2y} \right)^3 + \mathcal{O}(l^5). \quad (\text{C4})$$

While the third and fourth terms are the leading corrections due to the presence of salt, the two first terms can be related to half of the *exact nonlinear* Helmholtz free energy of two charged infinite planes in the presence of neutralizing counterions only (salt-free Gouy-Chapman case),

$$\frac{\beta F}{A} = \frac{1}{4\pi\ell_B} \left\{ \frac{2y^2}{L} - \frac{4}{\Lambda} \left[ 1 + \ln(\Lambda \sin y) + \frac{1}{2} \ln \left( \frac{2\pi\ell_B}{\zeta^3} \right) \right] \right\}, \quad (\text{C5})$$

where  $y$  is the solution of the transcendental equation  $y \tan y = L/\Lambda$ .

We define the extended Gouy-Chapman limit by truncating the above expansions, neglecting thus higher-order terms,

$$\omega_{\text{GC}}(\lambda, l) \equiv \frac{2y^2}{l} - \frac{4}{\lambda} \left[ 1 + \ln \left( \frac{\lambda}{2} \sin y \right) \right] + l - \frac{1}{2} \cot y \left( \sin^2 y + \frac{l}{\lambda} \right) \left( \frac{l}{2y} \right)^3, \quad (\text{C6})$$

$$\Pi_{\text{GC}}(\lambda, l) \equiv 2 \left( \frac{y}{l} \right)^2 - 1 + \frac{3(1 + \xi + \xi^2 y^2)(1 + \xi^2 y^2) + 2\xi^3 y^2}{16y^2(1 + \xi + \xi^2 y^2)(1 + \xi^2 y^2)} l^2, \quad (\text{C7})$$

where  $y = y(\xi)$  is the solution of the transcendental equation (C2).

## C.2 Extended large-separation limit

The large-separation osmotic-pressure asymptotics (B11) obtained in Appendix B.4 displays oscillations in the crossover ( $l \approx 1$ ) region. Because we want to match the linearized DH-like, the extended Gouy-Chapman and the large-separation asymptotic expressions at the crossover region, we need to find an extended expansion that does not display this shortcoming. In fact the pressure oscillations are avoided if one uses instead the implicit form  $l = l(\lambda, m)$ , which is obtained by expanding the eigenvalue equation,

$$l(\lambda, m) = \sqrt{m} K(m) - \sqrt{m} F[\arctan(\lambda/\sqrt{m}) | m], \quad (\text{C8})$$

in powers of  $(1 - m) \equiv t/(1 + t)$ . Accurate results in the crossover region, which will cover almost the whole  $(l \times \lambda)$  parameter space with logarithmic pressure deviations from the exact PB within 0.1%, are obtained by using fourth-order expansions of the elliptic integrals<sup>61</sup> about  $m = 1$ ,

$$\begin{aligned} K(m) &= \ln 4 - \frac{1}{2} \ln(1 - m) + \frac{1}{4}(1 - m) \left[ \ln 4 - 1 - \frac{1}{2} \ln(1 - m) \right] \\ &+ \frac{3}{128}(1 - m)^2 [6 \ln 4 - 7 - 3 \ln(1 - m)] + \frac{5}{1536}(1 - m)^3 [30 \ln 4 - 37 - 15 \ln(1 - m)] \\ &+ \frac{35}{196608}(1 - m)^4 [420 \ln 4 - 533 - 210 \ln(1 - m)] + \mathcal{O}[(1 - m)^5 \ln(1 - m)], \end{aligned} \quad (\text{C9})$$

$$\begin{aligned} F[\arctan(\lambda/\sqrt{m}) | m] &= F(\arctan \lambda | m) + \frac{\lambda(1 - m)}{2(1 + \lambda^2)^{7/2}} \left\{ (1 + \lambda^2)^3 \right. \\ &+ \frac{1}{4}(1 - m)(1 + \lambda^2)^2(3 - 2\lambda^4) + \frac{1}{24}(1 - m)^2(1 + \lambda^2)(15 + 5\lambda^2 - 10\lambda^4 + 6\lambda^6 + 9\lambda^8) \\ &\left. + \frac{1}{192}(1 - m)^3(105 + 70\lambda^2 - 70\lambda^4 + 28\lambda^6 + 66\lambda^8 - 72\lambda^{10} - 60\lambda^{12}) + \mathcal{O}[(1 - m)^4] \right\}, \end{aligned} \quad (\text{C10})$$

$$F(\arctan \lambda | m) = F(\arctan \lambda | 1) + \sum_{n=1}^{\infty} \frac{(m-1)^n}{n!} \frac{\partial^n F(\arctan \lambda | m)}{\partial m^n} \Big|_{m=1}$$

$$\begin{aligned}
&= \ln(\lambda + \sqrt{1 + \lambda^2}) + \frac{1-m}{4} \left[ \ln(\lambda + \sqrt{1 + \lambda^2}) - \lambda\sqrt{1 + \lambda^2} \right] \\
&+ \frac{3(1-m)^2}{64} \left[ 3 \ln(\lambda + \sqrt{1 + \lambda^2}) - \lambda\sqrt{1 + \lambda^2} (3 - 2\lambda^2) \right] \\
&+ \frac{5(1-m)^3}{768} \left[ 15 \ln(\lambda + \sqrt{1 + \lambda^2}) - \lambda\sqrt{1 + \lambda^2} (15 - 10\lambda^2 + 8\lambda^4) \right] \\
&+ \frac{35(1-m)^4}{49152} \left[ 105 \ln(\lambda + \sqrt{1 + \lambda^2}) - \lambda\sqrt{1 + \lambda^2} (105 - 70\lambda^2 + 56\lambda^4 - 48\lambda^6) \right] \\
&+ \mathcal{O}[(1-m)^5]. \tag{C11}
\end{aligned}$$

The asymptotic large-separation ( $l \rightarrow \infty$ ) excess semi-grand-canonical potential is obtained by integration of the osmotic-pressure difference,  $2t = -d\omega/dl$ ,

$$\begin{aligned}
\omega(\lambda, l) &= \omega(\lambda, \infty) - 2 \int_0^t d\tau \tau \frac{dl}{d\tau} + \mathcal{O}[(1-m)^6 \ln(1-m)] \\
&= \omega(\lambda, \infty) - 2tl + 2 \int_0^t d\tau l[\lambda, 1/(1+\tau)] + \mathcal{O}[(1-m)^6 \ln(1-m)] \\
&= \omega(\lambda, \infty) - \frac{2}{m} (1-m) l(\lambda, m) - 2 \int_1^m \frac{d\mu}{\mu^2} l(\lambda, \mu) + \mathcal{O}[(1-m)^6 \ln(1-m)]. \tag{C12}
\end{aligned}$$

We need to evaluate integrals of type

$$\int_1^m \frac{d\mu}{\mu^{3/2}} (1-\mu)^n, \quad \int_1^m \frac{d\mu}{\mu^{3/2}} \ln(1-\mu) (1-\mu)^n, \quad \text{for } n = 0, \dots, 4, \tag{C13}$$

which can all be performed analytically. After some algebraic manipulations, the last contribution of Eq. (C12) may be cast in the form

$$\begin{aligned}
2 \int_1^m \frac{d\mu}{\mu^2} l(\lambda, \mu) &= \frac{315}{32} \left[ \operatorname{arctanh} \sqrt{m} + \ln 2 - \ln(\lambda + \sqrt{1 + \lambda^2}) - \frac{19}{56} \right] - \frac{\lambda \mathcal{A}(\lambda)}{3360 (1 + \lambda^2)^{7/2}} + \frac{\mathcal{B}(m)}{8192 \sqrt{m}} \times \\
&\times \left[ \ln(1-m) - 4 \ln 2 + 2 \ln(\lambda + \sqrt{1 + \lambda^2}) \right] + \frac{\mathcal{C}(m)}{49152 \sqrt{m}} + \frac{\sum_{n=0}^7 \lambda^{2n+1} \mathcal{C}_n(m)}{430080 (1 + \lambda^2)^{7/2} \sqrt{m}}, \tag{C14}
\end{aligned}$$

$$\mathcal{A}(\lambda) = 34125 + 24150\lambda^2 - 56210\lambda^4 - 46480\lambda^6 + 9253\lambda^8 + 738\lambda^{10} - 5160\lambda^{12} + 1680\lambda^{14}, \tag{C15}$$

$$\mathcal{B}(m) = 25609 + 18404m - 4818m^2 + 1300m^3 - 175m^4, \tag{C16}$$

$$\mathcal{C}(m) = 123743 + 82792m - 56970m^2 + 16960m^3 - 2365m^4, \tag{C17}$$

$$\mathcal{C}_0(m) = 105 (14711 + 35356m - 11310m^2 + 3308m^3 - 465m^4), \tag{C18}$$

$$\mathcal{C}_1(m) = 70 (19795 + 26252m - 1254m^2 - 868m^3 + 235m^4), \tag{C19}$$

$$\mathcal{C}_2(m) = -70 (31873 + 98756m - 37826m^2 + 11636m^3 - 1655m^4), \tag{C20}$$

$$\mathcal{C}_3(m) = -560 (4129 + 7940m - 1730m^2 + 308m^3 - 23m^4), \tag{C21}$$

$$\mathcal{C}_4(m) = 156695 + 1690780m - 938350m^2 + 322924m^3 - 47665m^4, \tag{C22}$$

$$\mathcal{C}_5(m) = 79030 - 82600m + 186900m^2 - 111496m^3 + 22630m^4, \tag{C23}$$

$$\mathcal{C}_6(m) = -40 (4795 + 16940m - 7350m^2 + 2492m^3 - 365m^4), \tag{C24}$$

$$\mathcal{C}_7(m) = 1680 (35 + 140m - 70m^2 + 28m^3 - 5m^4). \tag{C25}$$

We may check numerically that the osmotic pressure  $2t$  corresponds indeed to the derivative of the excess grand potential  $\omega$  with respect to the semi-separation  $l$  between the two charged surfaces.

The extended large-separation expressions are obtained by truncating the above expressions, neglecting thus higher-order contributions. Collecting all contributions, the extended large-separation osmotic-pressure

difference  $\Pi_{\text{LS}} \equiv 2(1-m)/m$  is defined implicitly by the relation

$$\begin{aligned}
\frac{l(\lambda, m)}{\sqrt{m}} &= \ln 4 - \frac{1}{2} \ln(1-m) + \frac{1}{4}(1-m) \left[ \ln 4 - 1 - \frac{1}{2} \ln(1-m) \right] \\
&+ \frac{3}{128}(1-m)^2 [6 \ln 4 - 7 - 3 \ln(1-m)] + \frac{5}{1536}(1-m)^3 [30 \ln 4 - 37 - 15 \ln(1-m)] \\
&+ \frac{35}{196608}(1-m)^4 [420 \ln 4 - 533 - 210 \ln(1-m)] - \frac{\lambda(1-m)}{2(1+\lambda^2)^{7/2}} \left\{ (1+\lambda^2)^3 \right. \\
&+ \frac{1}{4}(1-m)(1+\lambda^2)^2(3-2\lambda^4) + \frac{1}{24}(1-m)^2(1+\lambda^2)(15+5\lambda^2-10\lambda^4+6\lambda^6+9\lambda^8) \\
&+ \left. \frac{1}{192}(1-m)^3(105+70\lambda^2-70\lambda^4+28\lambda^6+66\lambda^8-72\lambda^{10}-60\lambda^{12}) \right\} \\
&- \ln(\lambda + \sqrt{1+\lambda^2}) - \frac{1-m}{4} \left[ \ln(\lambda + \sqrt{1+\lambda^2}) - \lambda\sqrt{1+\lambda^2} \right] \\
&- \frac{3(1-m)^2}{64} \left[ 3 \ln(\lambda + \sqrt{1+\lambda^2}) - \lambda\sqrt{1+\lambda^2}(3-2\lambda^2) \right] \\
&- \frac{5(1-m)^3}{768} \left[ 15 \ln(\lambda + \sqrt{1+\lambda^2}) - \lambda\sqrt{1+\lambda^2}(15-10\lambda^2+8\lambda^4) \right] \\
&- \frac{35(1-m)^4}{49152} \left[ 105 \ln(\lambda + \sqrt{1+\lambda^2}) - \lambda\sqrt{1+\lambda^2}(105-70\lambda^2+56\lambda^4-48\lambda^6) \right], \quad (\text{C26})
\end{aligned}$$

with the associated semi-grand-canonical potential,

$$\omega_{\text{LS}}(\lambda, l) \equiv \frac{2}{\lambda} \operatorname{arccosh} \left( 1 + \frac{2}{\lambda^2} \right) + 4 \left( 1 - \frac{1}{\lambda} \sqrt{1+\lambda^2} \right) - \frac{2}{m} (1-m) l(\lambda, m) - 2 \int_1^m \frac{d\mu}{\mu^2} l(\lambda, \mu). \quad (\text{C27})$$

## D Globally self-consistent linearized equations

In this Appendix we show that the linearized equations that preserve the exact nature of the Legendre transformation do not lead to any improvements in the agreement between the linearized and nonlinear osmotic pressures in comparison to the linearized versions obtained in Section 3.

As discussed in detail in Appendix G of Ref. [1], the Legendre transformation between the semi-grand-canonical and the canonical descriptions of the system may be rendered *exact* if — instead of using the state-independent zero-th order Donnan densities (36) — one uses the quadratic truncation of the nonlinear averages, given by Eq. (38), as expansion densities to obtain the linearized functional. With the inclusion of the quadratic state-dependent contribution  $\langle \delta_2(x) \rangle$  to the average densities, we obtain the *globally* self-consistent linearized semi-grand-canonical potential and linearized osmotic-pressure difference,

$$\begin{aligned}
\hat{\omega}_{\text{DH}}(\lambda, l) &\equiv \frac{\kappa_{\text{b}}}{2n_{\text{b}}} \left[ \frac{\beta \hat{\Omega}_{\text{DH}}(\Lambda, L)}{A} + 2n_{\text{b}}L \right] = \frac{2}{\lambda} \left[ \operatorname{arctanh} \hat{\eta} - \frac{1}{\hat{\eta}} + \frac{1}{2} \hat{\eta} \hat{k} l \mathcal{L}(\hat{k}l) + \frac{1}{2\hat{\eta}} \langle \delta_2(x) \rangle \right] + l \\
&= \frac{2}{\lambda} \left\{ \operatorname{arctanh} \hat{\eta} - \frac{1}{\hat{\eta}} + \frac{5}{4} \hat{\eta} \hat{k} l \mathcal{L}(\hat{k}l) + \frac{1}{4} \hat{\eta} (\hat{k}l)^2 \left[ \mathcal{L}^2(\hat{k}l) - 1 \right] \right\} + l, \quad (\text{D1})
\end{aligned}$$

$$\begin{aligned}
\hat{\Pi}_{\text{DH}}(\lambda, l) &\equiv -\frac{d\hat{\omega}_{\text{DH}}(\lambda, l)}{dl} = \hat{k}^2 \left[ 1 + \hat{\eta} \delta_1(0) + \frac{1}{2} \delta_2(0) - \frac{1}{2} \langle \delta_2(x) \rangle \right] - 1 \\
&= \hat{k}^2 \left\{ 1 + \frac{1}{4} \hat{\eta}^2 \hat{k} l \mathcal{L}(\hat{k}l) + \frac{1}{4} (\hat{\eta} \hat{k} l)^2 \left[ \mathcal{L}^2(\hat{k}l) - 1 \right] \right\} - 1, \quad (\text{D2})
\end{aligned}$$

where the dimensionless parameters,

$$\hat{\eta} = \frac{1}{\sqrt{1 + (\lambda l/2)^2 e^{\langle \delta_2(x) \rangle}}}, \quad \hat{k}^2 = \sqrt{e^{\langle \delta_2(x) \rangle} + [2/(\lambda l)]^2} = \frac{e^{\langle \delta_2(x) \rangle/2}}{\sqrt{1 - \hat{\eta}^2}}, \quad (\text{D3})$$

are given implicitly in terms of the quadratic electrostatic-potential deviation,

$$\langle \delta_2(x) \rangle = \frac{1}{2} \hat{\eta}^2 \hat{k} l \left\{ 3 \mathcal{L}(\hat{k} l) + \hat{k} l \left[ \mathcal{L}^2(\hat{k} l) - 1 \right] \right\}. \quad (\text{D4})$$

To compute the linearized osmotic-pressure difference  $\hat{\Pi}_{\text{DH}}$ , Eq. (D2), one needs to take into account the total derivatives of the parametric forms, Eqs. (D3),

$$\begin{aligned} \frac{d}{dl} &= \frac{\partial}{\partial l} + \frac{d\hat{\eta}}{dl} \frac{\partial}{\partial \hat{\eta}} + \frac{d\hat{k}}{dl} \frac{\partial}{\partial \hat{k}} \\ &= \frac{\partial}{\partial l} - \frac{\hat{\eta}}{l} (1 - \hat{\eta}^2) \left( 1 + \frac{l}{2} \frac{d\langle \delta_2(x) \rangle}{dl} \right) \frac{\partial}{\partial \hat{\eta}} - \frac{\hat{k} \hat{\eta}^2}{2l} \left[ 1 - \frac{l}{2} \left( \frac{1 - \hat{\eta}^2}{\hat{\eta}^2} \right) \frac{d\langle \delta_2(x) \rangle}{dl} \right] \frac{\partial}{\partial \hat{k}}. \end{aligned} \quad (\text{D5})$$

In accordance to the infinite-separation linearized self-energy obtained in Section 3, the new version is also given by  $\hat{\omega}_{\text{DH}}(\lambda, l \rightarrow \infty) = 2/\lambda^2$ .

In Figures 1 and 2 we compare the two linearized osmotic-pressure definitions,  $\Pi_{\text{DH}}$  and  $\hat{\Pi}_{\text{DH}}$ , given by Eqs. (51) and (D2), with the exact nonlinear version  $\Pi$ , given by Eq. (33). The dotted lines in Figures 1 and 2 suggest a better agreement between the linearized osmotic-pressure difference  $\hat{\Pi}_{\text{DH}}$  and the full nonlinear counterpart  $\Pi$  — in comparison to the linearized version  $\Pi_{\text{DH}}$ , obtained in Section 3. However, as shown below by *explicit analytical* comparison, these *numerical* evidences are in fact misleading.

Asymptotic analytical expansions of the linearized osmotic-pressure difference  $\hat{\Pi}_{\text{DH}}$  about the weak-coupling ( $\ell_B \rightarrow 0$ ),

$$\begin{aligned} \hat{\Pi}_{\text{DH}} &= \Pi_{\text{DH}} + k^2 \left[ \frac{\eta^4}{16200} (\eta^2 + 5) (1 - \eta^2) k^8 l^8 + \mathcal{O}(k^{10} l^{10}) \right] = k^2 \left[ 1 - \frac{\eta^2}{6} k^2 l^2 - \frac{\eta^2}{90} (\eta^2 - 3) k^4 l^4 \right. \\ &\quad \left. + \frac{\eta^2}{945} (2\eta^2 - 5) k^6 l^6 - \frac{\eta^2}{113400} (7\eta^6 + 28\eta^4 + \eta^2 - 84) k^8 l^8 + \mathcal{O}(k^{10} l^{10}) \right] - 1, \end{aligned} \quad (\text{D6})$$

and the counterionic ideal-gas ( $L \rightarrow 0$ , finite  $\Lambda$ ) limits,

$$\hat{\Pi}_{\text{DH}} = \Pi_{\text{DH}} + \frac{2}{\lambda l} \left\{ \frac{\lambda^4}{675} \left( \frac{l}{\lambda} \right)^6 + \mathcal{O} \left[ (l/\lambda)^7 \right] \right\}, \quad (\text{D7})$$

show explicitly that both linearized osmotic pressures,  $\Pi_{\text{DH}}$  and  $\hat{\Pi}_{\text{DH}}$ , agree with the full nonlinear PB version  $\Pi$  up to the *same order* — cf. Eqs. (63) to (68). Therefore, the *numerical* indications of a better agreement of  $\hat{\Pi}_{\text{DH}}$ , as suggested by Figures 1 and 2, are purely *fortuitous*. In fact, for ratios  $\Lambda/L > 10^2$  (beyond the values shown in Figure 2) one observes a crossover between the deviations of the linearized versions,  $\Pi_{\text{DH}}$  and  $\hat{\Pi}_{\text{DH}}$ , with respect to the full nonlinear osmotic-pressure difference  $\Pi$ .

## References

- [1] M. N. Tamashiro and H. Schiessel, unpublished, preceding paper in this issue.
- [2] H. H. von Grünberg, R. van Roij, and G. Klein, *Europhys. Lett.* **55**, 580 (2001).
- [3] M. Deserno and H. H. von Grünberg, *Phys. Rev. E* **66**, 011401 (2002).
- [4] F. G. Donnan, *Chem. Rev.* **1**, 73 (1924).
- [5] J. Th. G. Overbeek, *Prog. Biophys. Biophys. Chem.* **6**, 57 (1956).
- [6] T. L. Hill, *Disc. Faraday Soc.* **21**, 31 (1956); *J. Phys. Chem.* **61**, 548 (1957).
- [7] V. Reus, L. Belloni, T. Zemb, N. Lutterbach, and H. Versmold, *J. Phys. II France* **7**, 603 (1997).
- [8] M. N. Tamashiro, Y. Levin, and M. C. Barbosa, *Eur. Phys. J. B* **1**, 337 (1998).

- [9] M. N. Tamashiro, E. Hernández-Zapata, P. A. Schorr, M. Balastre, M. Tirrell, and P. Pincus, *J. Chem. Phys.* **115**, 1960 (2001).
- [10] B. V. Derjaguin, *Kolloid-Z.* **69**, 155 (1934).
- [11] L. R. White, *J. Colloid Interface Sci.* **95**, 286 (1983).
- [12] J. N. Israelachvili, *Intermolecular and Surface Forces*, 2nd ed. (Academic Press, London, 1992).
- [13] D. Andelman, in *Handbook of Biological Physics*, edited by R. Lipowsky and E. Sackmann (Elsevier, Amsterdam, 1995) vol.1B, chapt. 12.
- [14] The Boltzmann-weighted equilibrium profiles (7) describe the ionic densities between the two charged plates. They do not apply to the infinite reservoir, that is only characterized by their associated (mean-field) ideal-gas microion chemical potentials,  $\beta\mu_{\pm} = \ln(n_{\text{b}}\zeta_{\pm}^3)$ . The equilibrium density profiles (7) were constructed in such a way to obey the charge-neutrality constraint (5), which implies an excess of counterions in the interplane region to neutralize the negative charge of the plates. This counterion excess is absent in the infinite salt reservoir. See also Section 2 of Ref. [1] for an explanation of the distinct roles attributed to the Lagrange multiplier  $\mu_{\text{el}}$  and the microion chemical potentials  $\mu_{\pm}$ , which are associated to different physical constraints of the problem, namely, the overall charge-neutrality constraint (5) and the electrochemical equilibrium with the infinite salt reservoir of bulk density  $n_{\text{b}}$ .
- [15] Because of the frequent use of the standard gauge ( $\mu_{\text{el}} \equiv 0$ ) the fact that this system constitutes a *Donnan equilibrium problem* has not been emphasized.
- [16] G. Gouy, *J. Phys. Paris* **9**, 457 (1910).
- [17] D. L. Chapman, *Philos. Mag.* **25**, 475 (1913).
- [18] *Higher Transcendental Functions*, Bateman Manuscript Project, edited by A. Erdélyi, W. Magnus, F. Oberhettinger, and F. G. Tricomi (McGraw-Hill, New York, 1953) vol.II.
- [19] *Handbook of Mathematical Functions*, edited by M. Abramowitz and I. A. Stegun (Dover, New York, 1970).
- [20] P. F. Byrd and M. D. Friedman, *Handbook of Elliptic Integrals for Engineers and Scientists*, 2nd ed. (Springer-Verlag, Berlin, 1971).
- [21] I. S. Gradshteyn and I. M. Ryzhik, *Table of Integrals, Series, and Products*, 5th ed., edited by Alan Jeffrey (Academic Press, San Diego, 1994).
- [22] E. J. W. Verwey and J. Th. G. Overbeek, *Theory of the Stability of Lyophobic Colloids* (Elsevier, Amsterdam, 1948).
- [23] R. J. Hunter, *Foundations of Colloid Science* (Clarendon Press, Oxford, 1987) vol.I, problem 7.3.10.
- [24] S. H. Behrens and M. Borkovec, *Phys. Rev. E* **60**, 7040 (1999).
- [25] We added a term  $2n_{\text{b}}L$  to  $\beta\Omega/A$ , which subtracts out the contribution from the infinite reservoir to the semi-grand-canonical potential. Therefore the *osmotic-pressure difference* between the interplane region and the salt reservoir is automatically obtained by taking the derivative of the excess semi-grand-canonical potential with respect to the semi-separation  $L$  between the charged planes, cf. Eq. (33).
- [26] Although the bare Coulomb interaction is long-ranged, even deionized aqueous suspensions at neutral pH characterized by small ionic strengths,  $n_{\text{b}} \approx 10^{-7}\text{M}$ , leads to Debye screening lengths of order  $\kappa_{\text{b}}^{-1} \approx 1\mu\text{m} \ll a$ . Therefore, for surfaces with curvatures of macroscopic size the applicability of the Derjaguin approximation is still valid.
- [27] R. A. Marcus, *J. Chem. Phys.* **23**, 1057 (1955).
- [28] H. Wennerström, B. Jönsson, and P. Linse, *J. Chem. Phys.* **76**, 4665 (1982).

- [29] E. Trizac and J.-P. Hansen, Phys. Rev. E **56**, 3137 (1997).
- [30] The nomenclature Debye-Hückel equation for Eq. (40) may be somewhat misleading, since it was obtained by a linearization of the mean-field PB functional, which *does not include* any microion-microion (in the interplane region or in the infinite reservoir) correlations. The original Debye-Hückel theory for symmetric electrolytes<sup>31,32,33,34</sup> takes these correlations automatically into account and leads to the famous electrostatic osmotic-pressure limiting law,  $-\kappa^3/(24\pi)$ . A more appropriate interpretation of the Debye-Hückel-like equation (40) is that it corresponds to an expansion about the infinite-temperature limit of the mean-field nonlinear PB equation.
- [31] P. W. Debye and E. Hückel, Phys. Z. **24**, 185 (1923).
- [32] T. L. Hill, *An Introduction to Statistical Thermodynamics* (Dover Publications, New York, 1986).
- [33] D. A. McQuarrie, *Statistical Mechanics* (Harper-Collins, New York, 1976).
- [34] Y. Levin, Rep. Prog. Phys. **65**, 1577 (2002).
- [35] The asymptotic expansions of the full nonlinear PB osmotic-pressure difference  $\Pi$ , obtained in Appendix B, provide higher-order terms and extend previous calculations by Pincus *et al.*<sup>36,13</sup> being in agreement with them except for the so-called Debye-Hückel region. In our notation, their osmotic-pressure asymptotic expressions for the different regimes read as follows. Counterionic ideal gas:  $\Pi = 2/(\lambda l)$ ; Gouy-Chapman:  $\Pi = (\pi/l)^2/2$ ; Intermediate ( $l \rightarrow \infty, \lambda \rightarrow 0$ ):  $\Pi = 32e^{-2l}$ ; Debye-Hückel ( $l \rightarrow \infty, \lambda \neq 0$ ):  $\Pi = 2/(\lambda \sinh l)^2$ . The two latter regimes are covered by the large-separation limit, Eq. (72).
- [36] P. Pincus, J.-F. Joanny, and D. Andelman, Europhys. Lett. **11**, 763 (1990).
- [37] H. L. Friedman and W. D. T. Dale, *Electrolyte solutions at equilibrium*, in *Statistical mechanics, Part A: Equilibrium techniques*, edited by B. J. Berne (New York, Plenum, 1977) chapt.3, pp.85.
- [38] L. Guldbbrand, B. Jönsson, H. Wennerström, and P. Linse, J. Chem. Phys. **80**, 2221 (1984).
- [39] M. J. Stevens and M. O. Robbins, Europhys. Lett. **12**, 81 (1990).
- [40] A. Diehl, M. N. Tamashiro, M. C. Barbosa, and Y. Levin, Physica A **274**, 433 (1999).
- [41] R. Kjellander and D. J. Mitchell, Chem. Phys. Lett. **200**, 76 (1992); R. Kjellander, *Distribution function theory of electrolytes and electrical double layers*, and references therein, in *Proceedings of the NATO Advanced Study Institute on Electrostatic Effects in Soft Matter and Biophysics*, edited by C. Holm, P. Kékicheff, and R. Podgornik (Kluwer, Dordrecht, 2001) pp.317.
- [42] M. Lozada-Cassou, W. Olivares, and B. Sulbarán, Phys. Rev. E **53**, 522 (1996).
- [43] I. Rouzina and V. A. Bloomfield, J. Phys. Chem. **100**, 9977 (1996).
- [44] B. I. Shklovskii, Phys. Rev. E **60**, 5802 (1999).
- [45] P. A. Pincus and S. A. Safran, Europhys. Lett. **42**, 103 (1998).
- [46] A. W. C. Lau, D. Levine, and P. Pincus, Phys. Rev. Lett. **84**, 4116 (2000); A. W. C. Lau, P. Pincus, D. Levine, and H. A. Fertig, Phys. Rev. E **63**, 051604 (2001); A. W. C. Lau, D. B. Lukatsky, P. Pincus, and S. A. Safran, *ibid.* **65**, 051502 (2002); A. W. C. Lau and P. Pincus, cond-mat/0209659.
- [47] B.-Y. Ha, Phys. Rev. E **64**, 031507 (2001).
- [48] M. N. Tamashiro and P. Pincus, Phys. Rev. E **60**, 6549 (1999).
- [49] Y. Burak and D. Andelman, J. Chem. Phys. **114**, 3271 (2001).
- [50] A. G. Moreira and R. R. Netz, Europhys. Lett. **52**, 705 (2000); Phys. Rev. Lett. **87**, 078301 (2001); R. R. Netz, Eur. Phys. J. E **5**, 557 (2001).

- [51] N. Grønbech-Jensen, R. J. Mashl, R. F. Bruinsma, and W. M. Gelbart, Phys. Rev. Lett. **78**, 2477 (1997).
- [52] R. Podgornik and V. A. Parsegian, Phys. Rev. Lett. **80**, 1560 (1998).
- [53] B.-Y. Ha and A. J. Liu, Phys. Rev. Lett. **79**, 1289 (1997); *ibid.* **83**, 2681 (1999); Y. Levin, J. J. Arenzon, and J. F. Stilck, *ibid.* **83**, 2680 (1999).
- [54] J. J. Arenzon, J. F. Stilck, and Y. Levin, Eur. Phys. J. B **12**, 79 (1999).
- [55] F. J. Solis and M. Olvera de la Cruz, Phys. Rev. E **60**, 4496 (1999).
- [56] B. I. Shklovskii, Phys. Rev. Lett. **82**, 3268 (1999).
- [57] J. J. Arenzon, Y. Levin, and J. F. Stilck, Physica A **283**, 1 (2000).
- [58] A. Diehl, H. A. Carmona, and Y. Levin, Phys. Rev. E **64**, 011804 (2001).
- [59] J. F. Stilck, Y. Levin, and J. J. Arenzon. J. Stat. Phys. **106**, 287 (2002).
- [60] M. Deserno, A. Arnold, and C. Holm, cond-mat/0206126.
- [61] We are presenting the expansions explicitly because algebraic-manipulation computer programs, like Mathematica and Maple, unfortunately do not perform series of the elliptic integrals with respect to the second argument  $m$ .

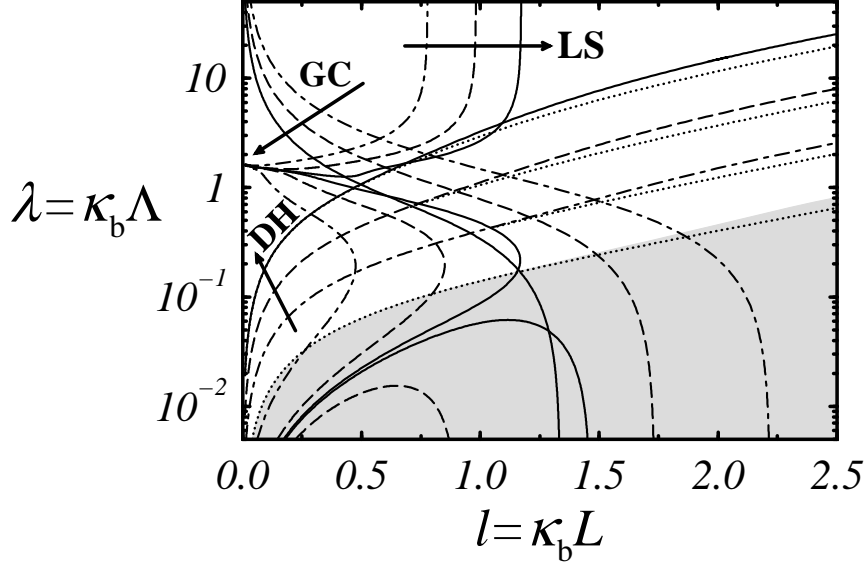


Figure 1: Logarithmic deviations from the PB of the different asymptotic osmotic-pressure differences. DH represents the Debye-Hückel-like, linearized-functional expansion about the weak-coupling limit, GC corresponds to the expansion about the salt-free Gouy-Chapman limit, and LS denotes the large-separation limit expansion. The region complementary to LS is splitted into three parts. In the gray region the linearized osmotic-pressure difference  $\Pi_{\text{DH}}$  becomes negative. The arrows indicate the direction of decreasing logarithmic deviation  $\delta\Pi$  from the PB results:  $10^{-1}$  (dot-dashed lines),  $10^{-2}$  (dashed lines),  $10^{-3}$  (solid lines). For comparison, we also display (dotted lines) the linearized results by including quadratic contributions in the expansion densities, as defined by the linearized pressure  $\hat{\Pi}_{\text{DH}}$ , Eq. (D2).

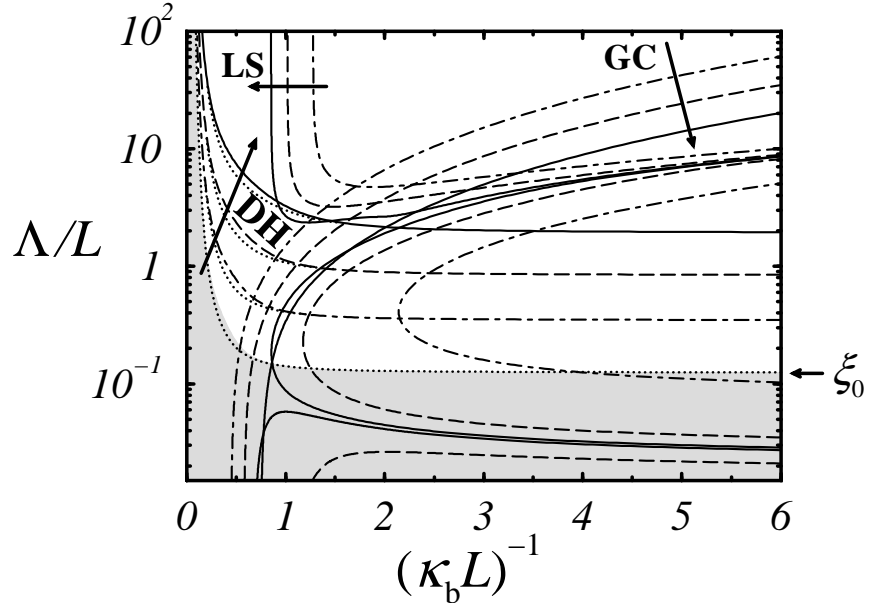


Figure 2: Same as in Figure 1, but plotted using different variables. At  $\kappa_b L \rightarrow 0$ , the  $\Pi_{\text{DH}} = 0$  line reaches the asymptotic value defined by Eq. (78),  $\xi_0 = \Lambda/L = 0.123863965 \dots$  Compare with Figure 1 from Ref. [36].

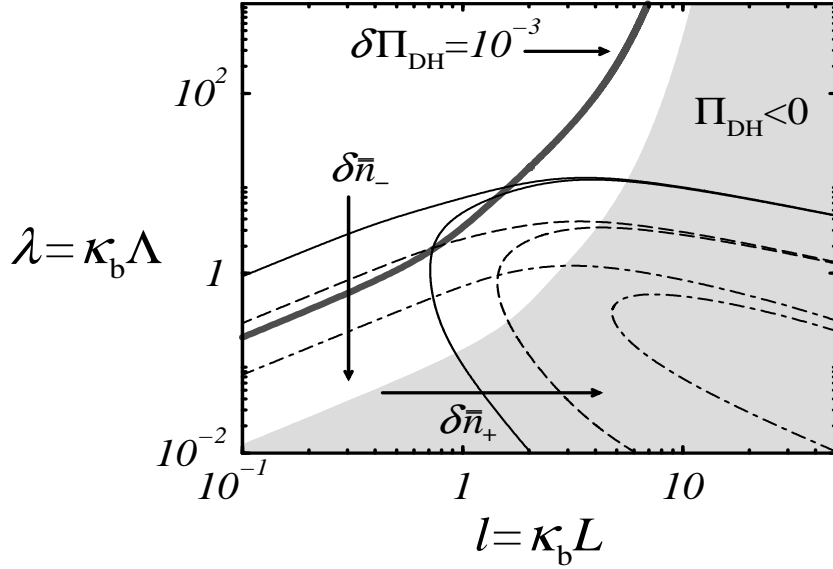


Figure 3: Deviations from the PB averaged densities of the state-independent zero-th order Donnan densities, which were used to perform the quadratic expansions of the nonlinear functional. The arrows indicate the direction of increasing logarithmic deviations  $\delta\bar{n}_{\pm}$  from the PB results:  $10^{-3}$  (solid lines),  $10^{-2}$  (dashed lines) and  $10^{-1}$  (dot-dashed lines). To allow a comparison with the region where the linearized theory breaks down, we also plotted the locus (dark gray thick line) where the logarithmic deviation from PB of the linearized osmotic-pressure difference is  $\delta\Pi_{\text{DH}} = 10^{-3}$ . In the light gray region the linearized osmotic-pressure difference becomes negative,  $\Pi_{\text{DH}} < 0$ . Although there is a close connection between this region and the increase of the deviations  $\delta\bar{n}_{\pm}$  for high-surface charges ( $\lambda \ll 1$ ), for low-surface charges ( $\lambda \gg 1$ ) and large separations ( $l \gg 1$ ), the linearized theory still predicts a negative linearized osmotic-pressure difference (upper-right region), while the full nonlinear one vanishes exponentially from positive values.